Imaging Neuroscience
an open access journal

Research Article

Mapping brain function underlying naturalistic motor observation and imitation using high-density diffuse optical tomography

Dalin Yang[a,*], Tessa G. George[a,*], Chloe M. Sobolewski[a], Sophia R. McMorrow[a], Carolina Pacheco[b], Kelsey T. King[a], Rebecca Rochowiak[c], Evan Daniels-Day[a], Sung Min Park[a], Emma Speh[a], Ari Segel[a], Deana Crocetti[c], Alice D. Sperry[c], Mary Beth Nebel[c], Bahar Tunçgenç[d], Rene Vidal[e], Natasha Marrus[f], Stewart H. Mostofsky[c,g,h], Adam T. Eggebrecht[a,i,j,k,l,m]

[a]Mallinckrodt Institute of Radiology, Washington University School of Medicine, St. Louis, MO, United States
[b]Department of Biomedical Engineering, Johns Hopkins University, Baltimore, MD, United States
[c]Center for Neurodevelopmental and Imaging Research, Kennedy Krieger Institute, Baltimore, MD, United States
[d]Department of Psychology, Nottingham Trent University, Nottingham, United Kingdom
[e]Department of Radiology, Perelman School of Medicine, University of Pennsylvania, Philadelphia, PA, United States
[f]Department of Psychiatry, Washington University School of Medicine, St. Louis, MO, United States
[g]Department of Neurology, Johns Hopkins University School of Medicine, Baltimore, MD, United States
[h]Department of Psychiatry and Behavioral Sciences, Johns Hopkins University School of Medicine, Baltimore, MD, United States
[i]Department of Biomedical Engineering, Washington University School of Engineering, St. Louis, MO, United States
[j]Division of Biology and Biomedical Sciences, Washington University School of Medicine, St. Louis, MO, United States
[k]Department of Physics, Washington University School of Arts and Science, St. Louis, MO, United States
[l]Department of Electrical and System Engineering, Washington University School of Engineering, St. Louis, MO, United States
[m]Department Imaging Sciences Engineering, Washington University School of Engineering, St. Louis, MO, United States

*Co-lead authors

Corresponding Author: Adam T. Eggebrecht (aeggebre@wustl.edu)

ABSTRACT

Autism spectrum disorder (ASD), a condition defined by deficits in social communication, restricted interests, and repetitive behaviors, is associated with early impairments in motor imitation that persist through childhood and into adulthood. Alterations in the mirror neuron system (MNS), crucial for interpreting and imitating actions, may underlie these ASD-associated differences in motor imitation. High-density diffuse optical tomography (HD-DOT) overcomes logistical challenges of functional magnetic resonance imaging to enable identification of neural substrates of naturalistic motor imitation. We aim to investigate brain function underlying motor observation and imitation in autistic and non-autistic adults. We hypothesize that HD-DOT will reveal greater activation in regions associated with the MNS during motor imitation than during motor observation, and that MNS activity will negatively correlate with autistic traits and motor fidelity. We imaged brain function using HD-DOT in N = 100 participants (19 ASD and 81 non-autistic individuals) as they engaged in observing or imitating a sequence of arm movements. Additionally, during imitation, participant movements were simultaneously recorded with 3D cameras for computerized assessment of motor imitation (CAMI). Cortical responses were estimated using general linear models, and multiple regression was used to test for associations with autistic traits, assessed via the Social Responsiveness Scale-2 (SRS-2), and imitation fidelity, assessed via CAMI. Both observing and imitating motor movements elicited significant activations in higher-order visual and MNS regions, including the inferior parietal lobule, superior temporal gyrus, and inferior frontal gyrus. Imitation additionally exhibited greater activation in the superior parietal lobule, primary motor cortex, and supplementary motor area. Notably, the right temporal–parietal junction exhibited activation during observation but not during imitation. Higher presence of autistic traits was associated with increased activation during motor observation in the

Received: 6 April 2025 Revision: 12 July 2025 Accepted: 18 August 2025 Available Online: 2 September 2025

right superior parietal lobule. No significant associations between brain activation and CAMI scores were observed. Our findings provide robust evidence of shared and task-specific cortical responses underlying motor observation and imitation, emphasizing the differential engagement of MNS regions during motor observation and imitation.

Keywords: autism spectrum disorder (ASD), non-autistic individuals (NAI), high-density diffuse optical tomography (HD-DOT), motor observation (OBS), motor imitation (IM), computer-vision-based assessment of motor imitation (CAMI)

1. INTRODUCTION

Autism spectrum disorder (ASD) is a neurodevelopmental condition characterized by deficits in social communication and enhanced presentation of restricted interests and repetitive behaviors, with heterogeneous traits across the population (Maenner, 2020; Mottron & Bzdok, 2020). Motor impairment is prevalent, with recent estimates suggesting this occurs in up to 88% of autistic children (Bhat, 2020; Licari et al., 2020; MacNeil & Mostofsky, 2012; Miller et al., 2021, 2024; Mostofsky et al., 2006). Impairments in motor imitation are particularly notable, as imitation is essential for early prosocial and language development (McAuliffe et al., 2020; Vivanti & Hamilton, 2014). Imitation across a range of communicative behaviors (e.g., vocalizations, arm gestures, facial expressions, and other non-verbal cues) is a key component of effective social interaction in neurotypical development (Taverna et al., 2021). Thus, early imitation deficits can hinder social development, and thereby social engagement and communication (Pittet et al., 2022; Yang et al., 2010). Additionally, individuals with ASD may experience difficulties in visual–motor integration, which supports the coordination of visual input with motor execution and is partially mediated by the mirror neuron system (MNS) (Nebel et al., 2016). Autistic individuals tend to rely more on proprioceptive inputs than visual cues than non-autistic peers when performing movements (Hirai et al., 2021; Marko et al., 2015). This increased reliance on proprioception could lead to differences in processing within sensory–motor integration systems, including cortical regions associated with visual processing, motor execution, visual attention, and association regions (Fuentes et al., 2011; Nebel et al., 2016). Such differences in processing may contribute to the observed motor imitation impairments in autistic individuals (Nebel et al., 2016). Therefore, a deeper understanding of the brain function underlying both observation and imitation of natural motor movements is crucial for developing targeted interventions to improve social engagement, communication, and outcomes for autistic and neurotypical individuals.

The current standard in traditional approaches for imitation assessment involves human observation coding (HOC), which introduces bias and requires extensive training (Santra et al., 2025; Tuncgenc et al., 2021), thereby making it impractical for use in clinics and home settings. Developing an automatic assessment is valuable but challenging, as human motion is highly heterogeneous and involves spatial and temporal aspects. Accurately capturing subtle changes in imitation is essential for assessing imitation deficits related to autism. Addressing this, Tuncgenc et al. (2021) developed an automatic, Computerized Assessment of Motor Imitation (CAMI) that utilizes metric learning and dynamic time warping for precise measurement of motor imitation fidelity (Tuncgenc et al., 2021). CAMI quantifies spatio-temporal differences between the movements of a participant and that of a gold standard (Celebi et al., 2013) and has been validated as a reliable method for assessing motor imitation in school-age children, with CAMI-generated scores being strongly correlated with traditional labor-intensive, subjective HOC-based methods (Lidstone et al., 2021; Tuncgenc et al., 2021). Crucially, CAMI methods have proven to be better than HOC at discriminating autistic from non-autistic children, including neurotypical children and those with attention-deficit/hyperactivity disorder (ADHD) (Santra et al., 2025). Additionally, CAMI scores have been shown to significantly correlate with measures of autism trait severity (using the Social Responsiveness Scale, 2nd Edition [SRS-2] (Constantino et al., 2003), a well-established clinical metric of autistic traits). Together, these findings demonstrate that CAMI can detect motor imitation difficulties that are specific to autism.

While CAMI has shown promise in detecting diagnostic differences in motor imitation fidelity, the relationships between variability in brain function and naturalistic motor imitation fidelity remain unknown (Zhao et al., 2023). Elucidating patterns of brain function underlying motor imitation behaviors may help parse observed heterogeneity in ASD (Latreche et al., 2024; Pittet et al., 2022), point to neural mechanisms that lead to deficits in motor imitation, and guide more individualized treatment planning (Dapretto et al., 2006; Rogers & Vismara, 2008). The main challenges are due to the physical constraints and limitations of neuroimaging modalities such as functional magnetic resonance imaging (fMRI) (Crone et al., 2010; Scarapicchia et al., 2017). Specifically, the MRI environment requires

participants to lay supine in a small bore that inherently restricts studies to small-scale movements, such as those of fingers or hands, and it is incompatible with capturing brain function during more general, naturalistic motor behaviors (Chaminade et al., 2005). In contrast, high-density diffuse optical tomography (HD-DOT) provides a naturalistic and open scanning environment that enables the assessment of brain function across the lifespan (Chitnis et al., 2016; Eggebrecht et al., 2014; Ferradal et al., 2016; Habermehl et al., 2012; Zeff et al., 2007), in school-age autistic children (Eggebrecht et al., 2014; Fishell et al., 2019; Hassanpour et al., 2017; McMorrow et al., 2025; Yang et al., 2024), and in bedside clinical settings such as intensive care units (McMorrow et al., 2025). Importantly, HD-DOT provides signal-to-noise, anatomical specificity, and spatial resolution approaching that of fMRI (Eggebrecht et al., 2012; Ferradal et al., 2014; Sherafati et al., 2020). Additionally, HD-DOT provides higher spatial resolution (Fan et al., 2025; Markow et al., 2025; White & Culver, 2010) and improved depth sensitivity over a broader cortical field of view than traditional functional near-infrared spectroscopy (fNIRS) methods (Eggebrecht et al., 2012; Fishell et al., 2020). While previous foundational studies using wearable fNIRS have opened the door to measuring brain function during natural interactions in young children who go on to develop autism (Blanco et al., 2023; Frijia et al., 2021), more recent advancements in wearable HD-DOT systems (Collins-Jones et al., 2024; Uchitel et al., 2023) highlight the potential for high-fidelity optical neuroimaging to be deployed in both clinic and home settings (Mcmorrow et al., 2025; Uchitel et al., 2022). Given previous success using HD-DOT to map brain function during observation of biological motion (Yang et al., 2024) in children with and without autism, herein, we conducted a proof-of-principle study using HD-DOT to detect and localize cortical brain function underlying naturalistic gross motor imitation.

Extant human neuroimaging studies using fMRI suggest motor imitation relies on the MNS, which encompasses the ventral premotor cortex (vPMC), supplementary motor area (SMA), and inferior and superior parietal lobules (IPL and SPL, respectively) (Iacoboni & Dapretto, 2006; Williams et al., 2001). These regions, which significantly overlap with praxis networks (Michalowski et al., 2022; Rosenzopf et al., 2022), are crucial for visual–motor integration, that is, for encoding observed actions and translating them into motor execution. Additionally, the superior temporal sulcus (STS) can be considered part of the MNS, as it plays a role in self-other mapping, facilitating action recognition and intention understanding (Buccino et al., 2004; Iacoboni et al., 2005; Rizzolatti & Craighero, 2004; Williams et al., 2001). The MNS activates not only when individuals perform an action but also when they observe someone else performing that action (Cattaneo & Rizzolatti, 2009; Dushanova & Donoghue, 2010; Iacoboni & Dapretto, 2006; Kana et al., 2011), highlighting the importance of this network in developing abilities to replicate another's movements and understanding and interpreting the actions of others (Buccino et al., 2004; Iacoboni & Dapretto, 2006; Iacoboni et al., 2005; Kemmerer, 2021; Rizzolatti & Craighero, 2004; Umiltà et al., 2001; Williams et al., 2001). Autism-associated differences in MNS activity have been observed during motor imitation and action observation (Dapretto et al., 2006; Datko et al., 2018; Falck-Ytter et al., 2006; Iacoboni et al., 2005; Lust et al., 2019; Oberman et al., 2008; Raymaekers et al., 2009; Tylen et al., 2012; Wadsworth et al., 2018), with autistic individuals exhibiting reduced MNS activation, impairments in understanding action intentions, and deficits in action prediction (Dapretto et al., 2006; Falck-Ytter et al., 2006; Iacoboni et al., 2005). Additionally, electroencephalogram (EEG) and fMRI studies found atypical mu suppression, altered neural mirroring, and reduced engagement during social interactions (Oberman et al., 2008; Raymaekers et al., 2009; Tylen et al., 2012). These findings suggest that MNS dysfunction contributes to the social and motor impairments often observed in autistic individuals. Further, the variability in MNS activation has been shown to correlate with autistic traits, suggesting the MNS may underlie key behavioral variability associated with ASD (Wymbs et al., 2021).

Accurate motor imitation also relies on one's ability to efficiently detect and shift attention to others' actions, which relies on a ventral attention network (VAN) comprising the temporoparietal junction (TPJ) and ventral prefrontal cortex (Corbetta et al., 2008; Hsu et al., 2020). Further, imitation requires proper application of goal-directed attention and action planning, which relies on a dorsal attention network (DAN) comprising the middle temporal V5 area, the intraparietal sulcus (IPS), and frontal eye fields (FEF) regions (Corbetta & Shulman, 2002; He et al., 2007; Marco et al., 2011; Nardo et al., 2011; Scassellati, 1999). Difficulties with shifting attention and with goal-directed planning are often reported features of ASD (Geurts et al., 2004; Ozonoff et al., 1991); as such, abnormal activity of MNS with VAN and DAN may help explain deficits in imitation skills and related behaviors observed in many autistic individuals.

In this study, we used simultaneous HD-DOT and CAMI to investigate how variability in brain function relates to movement observation and imitation fidelity in a sample of autistic and non-autistic adults. Extant literature has largely focused on fine-motor task-based fMRI studies, providing limited insight into the neural activity underlying gross motor observation and imitation in the general population, as gross motor skills could contribute

to development of gestures and important for social interaction. Hence, the objective of this study is to address this gap by using limb/truncal movements to assess motor imitation fidelity using CAMI while leveraging HD-DOT to capture the neural correlates of observation and imitation of these movements. Regarding CAMI, we hypothesize that participants in the ASD group will have lower imitation fidelity scores than non-autistic participants. Regarding HD-DOT, we hypothesize that observing and imitating will engage MNS regions including premotor, parietal, and temporal brain regions, with primary motor regions additionally engaged during imitation compared with the resting state. We also hypothesize that regions within the DAN and VAN will be activated both when observing and imitating movements, with stronger brain activation within key regions of the DAN and MNS during motor imitation. Last, we hypothesize that brain response strength within the MNS will be negatively correlated with dimensional measures of autistic traits (i.e., SRS-2 T-scores) during observation and imitation, and positively correlated with imitation fidelity (i.e., CAMI scores) during motor imitation.

2. MATERIAL AND METHODS

2.1. Participants

We recruited 100 participants (age 30.15 ± 12.97 years, 45 male/55 female, 18 ASD participants, Table 1) from the St. Louis, Missouri metropolitan community. The final sample that went into analyses was reduced following exclusions after data quality checks and missing data, as detailed in the Statistical Analyses section below. All participants gave written informed consent to participate in this study, which was approved and carried out in accordance with the Human Research Protection Office at Washington University School of Medicine. All autistic participants had a prior diagnosis from a physician. In the non-autistic individual (NAI) group, the right- to left-handedness ratio was 71:7, while in the ASD cohort, it was 16:3. The population-wide ratio is 9:1 (Papadatou-Pastou et al., 2020). Additionally, three NAI participants did not report their handedness status.

2.2. Observation and imitation tasks

The motor observation and motor imitation tasks each consisted of 6 different movement sequences separated by 30-second inter-stimulus intervals (ISIs; Fig. 1). Data collected during these ISIs were treated as resting-state periods and used to contrast against task-related activation. The movement sequences lasted 16–21 seconds and comprised 14–18 individual movement types, which were unfamiliar, did not have an end goal, and required moving both arms simultaneously while the participants were seated in a chair. These movements were selected based on prior research indicating that autistic participants experience difficulties performing them (Tuncgenc et al., 2021). For the observation task, participants were instructed to passively watch the movement sequences and to remain as still as possible. For the motor imitation task, participants were instructed to mirror the actor's arm movements as accurately as possible while limiting their head motion (Fig. 1). In our protocol, each participant completed at least one observation run and one imitation run (i.e., ~316 seconds per run). If the participant remained engaged, participants were asked to complete

Table 1. Participant demographics and group characteristic.

Measure		Full Sample NAI (n = 81)			Full Sample ASD (n = 19)			Statistic (*z*)	*p*-value
Sex, Males:Females		33:48			12:7			-	0.12
Handedness, R:L*		71:7			16:3			-	0.41
Race, A:B:M:W:U**		16:0:3:60:1			1:2:1:14:1			-	
Ethnicity, H:N:U***		4:76:1			1:17:1			-	
		Means	*S.D.*	*n*	*Means*	*S.D.*	*n*	-	-
Age, years, [range]		27.56	9.36	81	31.47	16.73	19	1.37	0.17
SRS-2	Raw score	43.61	24.68	74	82.94	33.72	17	-	-
	T-score	51.07	8.67	74	65.00	11.89	17	4.44	<0.001
KBIT-2 IQ	Verbal	113.38	17.22	67	103.39	20.04	18	-	-
	Nonverbal	117.61	11.97	67	110.67	16.82	18	-	-
	Full scale	117.75	13.69	67	107.83	19.77	18	1.52	0.14
CAMI	Score	0.52	0.21	74	0.31	0.26	16	3.28	0.001

*Handedness: Right (R), Left (L).
**Racial group: White (W), Asian (A), more than one race (M), Black (B), and Unknown (U).
***Ethnical group: Not Hispanic/Latino (N), Hispanic/Latino (H), Unknown (U).

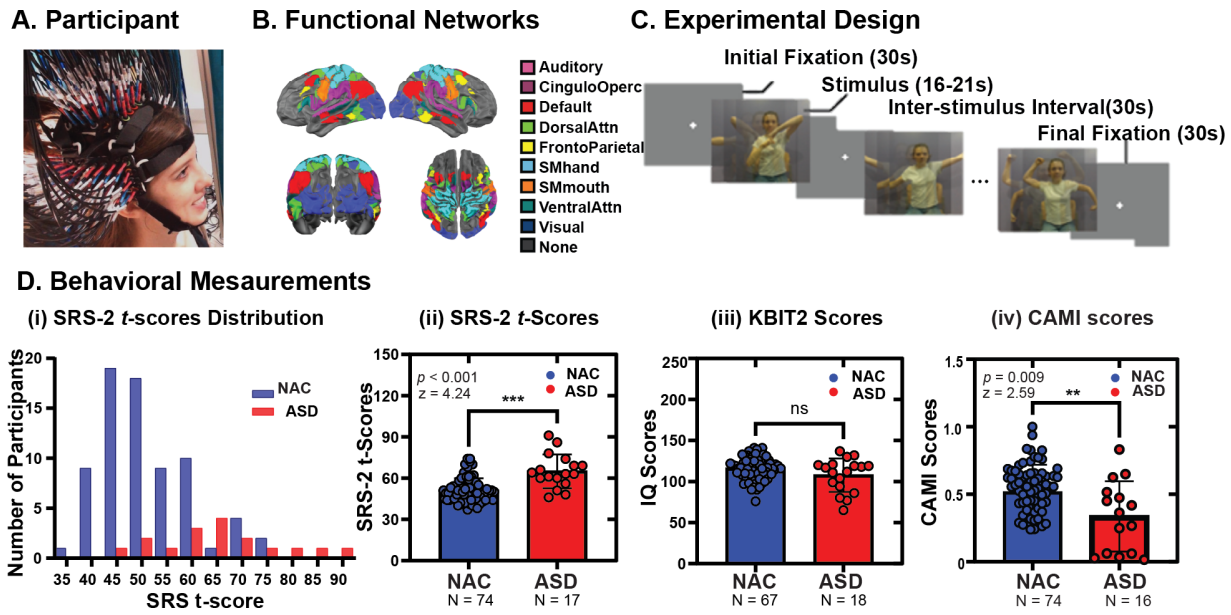

Fig. 1. Study Design and Behavioral Assessments. (A) Participant wearing the HD-DOT cap. (B) Field of view from dorsal, posterior, and lateral perspectives and overlapping Gordon parcels colored by functional networks assignment. (C) Experimental design for the motor observation and imitation tasks. (D) Behavioral assessments including SRS-2 scores, KBIT-2, and CAMI scores.

additional imitation and observation runs. Stimuli were presented via the Psychophysics toolbox 3 for MATLAB using custom-built scripts. All movements were performed by the same seated female actor and the stimuli were displayed on a 69 cm monitor placed 110 cm from the nasion in front of the participant. Participant brain function was recorded with HD-DOT during all observation and imitation tasks. Participant imitation fidelity was measured with CAMI using the participants' motion data recorded during the imitation task. Motion data were recorded using an Xbox Kinect 3D camera located on top of the stimulus presentation monitor and iPi Recorder (iPiSoft4, Moscow, Russia).

2.3. HD-DOT system

The continuous-wave HD-DOT system has been previously described (Tripathy et al., 2024) and comprised 128 dual-wavelength optical sources with wavelengths of 685 and 830 nm, and 125 avalanche-photodiode detectors. The imaging cap supported multiple source–detector distances (i.e., 11, 24, 33, and 40 mm), providing over 3,500 measurement pairs per wavelength for image reconstruction at a 10 Hz frame rate. To compute cortical sensitivity across the HD-DOT field of view, we used NIRFASTer to model fluence in the head. Based on the anatomical registration of the optode array, the sensitivity profile for each source–detector pair was calculated and then a flat-field reconstruction was estimated to provide a system field of view based on a binarized flat-field threshold of 10% (Fan et al., 2025). While the optode layout (Fig. 1A) includes a physical separation of approximately 1–2 cm between the temporal and parietal pads, the sensitivity profiles of source–detector measurement pairs that span that gap effectively bridge inter-pad distances, resulting in continuous cortical sensitivity across the surface, as illustrated in the combined sensitivity map (Fig. 1B). The HD-DOT field-of-view covered continuous aspects of temporal, occipital, parietal, and prefrontal cortical areas (Fig. 1A, B). To optimize HD-DOT cap fitting, we utilized anatomical landmarks (e.g., tragus, inion, and nasion) for precise cap alignment. For participants with long hair, the hair on top was parted down the middle and secured into two tight ponytails positioned at the back of the head to minimize interference with the optodes. Participants were then instructed to comb the optodes through their hair until they made even contact with the scalp across the sides and back of the cap. We then secured the cap symmetrically by aligning it with the tragus and fiducials on the cap. Finally, we adjusted the optodes to ensure optimal scalp contact, guided by real-time readouts of data quality metrics such as coupling coefficients, noise levels, and the mean light level for each measurement plotted against source–detector separation distance (Fishell et al., 2020).

2.4. Behavioral assessments

The Social Responsiveness Scale, 2nd Edition (SRS-2), provided a measure of quantitative autistic traits, with

higher scores corresponding to higher levels of autism traits and lower levels of social reciprocity. SRS-2 scores are continuously distributed throughout the general population. The SRS-2 raw scores were generated based on adult self-report form, and sex-normed SRS-2 T-scores were used in analyses. Participant handedness was determined by the Edinburgh Handedness Inventory (EHI) (Oldfield, 1971). Measures of verbal and non-verbal intelligence quotients (IQ) were assessed with the Kaufman Brief Intelligence Test-2 (KBIT-2) (Pitts & Mervis, 2016). All participants had a composite IQ or verbal IQ > 80.

The CAMI algorithm, described previously (Tuncgenc et al., 2021), was modified for this study to allow for the imitation task to be used while participants were seated in our fiber-based HD-DOT system. The seated CAMI algorithm considered joints from the upper body as there was no involvement of the lower limbs; all other features of the CAMI analyses remained the same as the previously described methods. The spatial coordinates of 20 joints were extracted from the Xbox Kinect 3D motion sensor depth recordings using iPi Motion Capture Software (iPiSoft 4.6.2, Moscow, Russia). Calculation of CAMI scores consisted of five main steps: (1) preprocessing, (2) automatic joint importance estimation, (3) calculation of the distance feature, (4) calculation of the time features, and (5) calculation of the CAMI score. Preprocessing consisted of (i) defining the hip position as the origin, mapping the sequence of movements to a skeleton of fixed size, (ii) correcting the initial orientation of the participant to match that of the actor (Supplementary Fig. S1B), and (iii) correcting the average position of the participants' joints associated with their spine (hip, lower spine, middle spine, and neck) to match those of the average position of the gold standard (Supplementary Fig. S1C). This alignment step was completed to avoid penalizing participants for their initial posture or sitting position in the cap, as this could vary between participants. The CAMI algorithm yielded an imitation fidelity score ranging between 0 and 1, with higher scores indicating higher fidelity.

2.5. Data pre-processing and image reconstruction

HD-DOT data were pre-processed using the NeuroDOT toolbox in MATLAB (https://www.nitrc.org/projects/neurodot). Each of the raw source–detector pair light level measurements was converted to optical density by calculating the log-ratio of the raw measurement data relative to its temporal mean. Measurements with greater than a 7.5% temporal standard deviation in the least noisy (lowest motion) 60 seconds of each run were removed from further analyses. Data were bandpass filtered between 0.02 and 1.0 Hz using 9-pole Butterworth filters. Then, the superficial signal for each wavelength was estimated as the average across the closest nearest neighbor measurements (11 mm S-D pair separation) and regressed from all measurement channels (Gregg et al., 2010). The optical density time traces were then low pass filtered with a cutoff frequency of 0.15 Hz to attenuate high-frequency nuisance signals from physiological sources such as cardiac pulsation (~1 Hz) and respiration (~0.2–0.4 Hz). This conservative cutoff was chosen to preserve the slow task-evoked hemodynamic responses associated with our block-design paradigm (16–21 seconds task periods followed by 30 seconds rest), in which neural responses are expected to occur primarily below 0.1 Hz. As previously described (Yang et al., 2024), a wavelength-dependent sensitivity matrix was computed and inverted to calculate relative changes in absorption at the two wavelengths via reconstruction using a Tikhonov regularization parameter of 0.01 and spatially variant regularization parameter of 0.1. Relative changes in the concentrations of oxygenated, deoxygenated, and total hemoglobin were obtained from the absorption coefficient changes by the spectral decomposition of the extinction coefficients of oxygenated and deoxygenated hemoglobin at the two wavelengths (i.e., 685 and 830 nm). All data were resampled to a $1 \times 1 \times 1$ mm^3 standard MNI atlas using a linear affine transformation for statistical analyses.

2.6. Data quality assessment and motion censoring

Quantitative data quality assessments included the percentage of good measurements (GM) retained (Yang et al., 2024) and the median pulse band signal-to-noise ratio (SNR) (Fishell et al., 2020; Yang et al., 2024). As previously described (Yang et al., 2024), runs with GM < 80% and/or SNR < 1.0 were excluded from further analysis to ensure robust data reliability. Global variance in the temporal derivative (GVTD) was used to detect and censor time points with motion-driven artifact in the data (Schroeder et al., 2023; Sherafati et al., 2020; Yang et al., 2024). Briefly, GVTD is calculated as the RMS of the first temporal derivative across the set of first nearest-neighbor measurements for each time point. Higher GVTD values indicate higher global variance in the optical time course and are exquisitely sensitive to motion-based changes in optode–scalp coupling. Motion censoring with GVTD excludes the time points that exceed the GVTD noise threshold. We used a stringent GVTD threshold of 0.1% based on previous studies utilizing GVTD-based motion censoring (Yang et al., 2024).

2.7. Statistical analyses

2.7.1. Behavioral and demographic measurements

We tested for potential group differences (ASD vs. NAI) in age, SRS-2, KBIT-2, and CAMI scores using Wilcoxon Rank-Sum test, as Shapiro–Wilk tests indicated non-normal distribution. Effect sizes were reported using Rank–Biserial correlation (r), which measures significance based on rank for a non-parametric test. Differences in sex and handedness were tested with Fisher's exact test. To test for group differences in SRS-2 and CAMI scores while controlling for demographic variables, we used analysis of covariance (ANCOVA) to further conduct hypothesis tests to investigate for significant differences including age, sex, and handedness as covariates and group index as a fixed factor. Type III Sum of Squares was employed to address potential biases due to unbalanced data and to ensure that covariates were appropriately controlled. Due to the missed handedness (ANCOVA-SRS-2 = 1, ANCOVA-CAMI = 3), there were 90 participants (i.e., 17 ASD and 73 NAI) and 87 participants (i.e., 17 ASD and 73 NAI) used for ANCOVA-SRS and ANCOVA-CAMI tests, respectively. To test the relationship between autistic traits (SRS-2 scores) and imitation fidelity (CAMI scores), we conducted multiple regression analyses for each group. In this study, 83 participants had both CAMI and SRS-2 scores (i.e., 14 ASD and 69 NAI). Furthermore, we used one-way ANOVA and post-hoc t-tests to examine the impact of race and ethnicity on the data quality (i.e., median SNR and GM) for all 100 participants across 5 racial (White n = 75, Asian n = 17, more than one race n = 4, Black n = 2, and unknown n = 2) and 3 ethnic groups (not Hispanic/Latino n = 93, Hispanic/Latino n = 5, unknown n = 2).

2.7.2. Data inclusion criteria

After pre-processing and data quality assessment, 78 participants (i.e., 13 ASD and 65 NAI) were identified as having high-quality (i.e., GM > 80%, SNR > 1) observation task data, while 64 participants (i.e., 13 ASD and 51 NAI) had high-quality imitation task data meeting data quality assessment thresholds described in the previous section. Additionally, one participant was excluded due to technical issues with the stimulus presentation. As a result, the final sample consisted of n = 77 participants (i.e., 13 ASD and 64 NAI) for motor observation analysis and n = 63 participants (i.e., 13 ASD and 50 NAI) for motor imitation analysis. Further, 9 participants were missing SRS-2 scores and 21 participants were unable to finalize KBIT-2 testing due to non-native English speaking and scheduling difficulties. Therefore, in our final brain–behavior association analyses, n = 71 participants (i.e., 13 ASD and 58 NAI) had SRS-2 scores and passed data quality thresholds for the observation task, and n = 55 participants (i.e., 12 ASD and 43 NAI) had SRS-2 scores and passed data quality threshold for the imitation task. For the CAMI analyses, out of 100 participants, n = 89 CAMI scores (i.e., 17 ASD, 72 NAC) were valid after exclusion due to damaged video files (n = 6), no video recording (n = 2), or preprocessing issues with the CAMI data (n = 3). Additionally, to avoid possible practice effects from the first imitation run of the motor imitation task, we focus brain–behavior analyses on those 48 participants (i.e., 11 ASD and 37 NAC) whose HD-DOT data passed data quality thresholds in the first imitation run. Supplementary Table S1 provides a detailed summary of participant inclusion and retention across each analysis step, highlighting modality-specific exclusions and final group-specific sample sizes for brain–behavior analyses.

2.7.3. Brain activation estimation

We used general linear model (GLM) analyses to estimate the brain response to each task (observation or imitation) using a canonical hemodynamic responses function (HRF) based on HD-DOT data (Hassanpour et al., 2014). We present the relative changes in oxygenated hemoglobin (HbO) results as HbO signals exhibit a higher contrast-to-noise ratio than deoxygenated hemoglobin (HbR) or total hemoglobin (HbT) (Eggebrecht et al., 2014; Schroeder et al., 2023; Yucel et al., 2021). We used the Gordon cortical parcellation (Gordon et al., 2016) to provide an unbiased spatial sampling for hypothesis-driven analyses. The functionally defined Gordon parcellation provided a framework to couch our analyses within functionally identified parcels of interest. The intersection of each Gordon parcel with the HD-DOT field of view provided 192 parcels associated with 9 functional networks (i.e., auditory, frontal-parietal, default mode, dorsal-attention, somatosensory hand, somatosensory mouth, ventral attention, cingulo-opercular, and visual functional networks; Fig. 1B). Small parcels of size <500 mm^3 (approximately equivalent to a 5 mm spherical seed) were excluded from analyses, providing a final parcel count of 118. Based on the Euclidean mean Montreal Neurological Institute (MNI) coordinate of each parcel location and its associated Brodmann area (BA), we a *priori* selected 58 parcels located in premotor cortex (BA6), inferior parietal lobule (BA39 and 40), inferior frontal gyrus (BA44 and 45), pre-supplementary (BA6), and primary motor area (BA4). This parcel selection was defined prior to data analysis to ensure an anatomically grounded and literature-informed representation of the mirror neuron system (MNS) (Iacoboni & Dapretto, 2006; Kemmerer, 2021; Rizzolatti & Craighero, 2004). For the within-task statistics, we used

two-tailed paired t-tests to compare the task effect (i.e., observation or imitation) with rest (i.e., ISI), thresholding with $p < 0.05$ and a false discovery rate (FDR) correction. We used two-sample t-tests to compare contrast effects between motor observation and motor imitation, with $p < 0.05$ with an FDR correction. Additionally, Cohen's D was used to measure effect size for the contrasts, including observation versus rest, imitation versus rest, and observation versus imitation. In this study, we first performed brain-wide analyses to test for significant activations during motor observation and imitation. We also investigated which regions were significantly active more during observation versus imitation. We then highlighted how significantly activated regions are represented within key brain networks previously implicated in observing or imitating motor movements (i.e., MNS, DAN, VAN). Finally, we investigated whether cortical activations during observation were associated with SRS-2 scores and whether cortical activations during imitation were associated with either SRS-2 scores or simultaneously measured imitation fidelity (CAMI scores).

2.7.4. Brain–behavioral association analysis

We calculated Pearson correlations between the parcel-specific brain responses to motor observation and motor imitation with the SRS-2 T-scores to investigate brain–behavior correlations relative to autistic traits. We also calculated the Pearson correlation between the motor imitation responses and the CAMI scores to assess brain–behavior relationships relative to motor imitation fidelity. Further, we used multiple regression analysis to examine how demographic factors (i.e., age, sex, and handedness) might affect the correlation between above brain and behavioral associations. More specifically, we assessed the effects of sex, age, and handedness, along with behavioral measurements (i.e., SRS-2 or CAMI scores), using brain activation data that passed the $p < 0.05$ threshold (with and without FDR correction) as the dependent variables. Overall, Pearson correlation is helpful for understanding fundamental relationships between brain and autistic traits (SRS-2 T-scores and CAMI scores), while multiple regression provides a more comprehensive perspective, accounting for all potential effects of multiple demographic predictors (i.e., age, sex, and handedness) and autistic traits (SRS-2 T-scores and CAMI scores).

3. RESULTS

3.1. Behavioral measures

The participant demographics and group characteristics are listed in Table 1. In our samples, autistic participants exhibited significantly higher scores on the SRS-2 than non-autistic individuals (NAI; Fig. 1D i, ii; NAI $n = 74$, ASD $n = 17$, $z = 4.24$, $r = 0.91$, $p < 0.001$). There were no significant differences between the NAI and ASD groups in verbal or non-verbal KBIT-2 scores (Fig. 1D iii; NAI $n = 67$, ASD $n = 18$, $z = 1.29$, $r = 3.98$, $p = 0.20$). In line with previous CAMI studies and our hypothesis, the NAI group exhibited significantly higher CAMI scores than the ASD participants (Fig. 1D iv; NAI $n = 74$, ASD $n = 16$, $z = 2.59$, $r = 5.41$, $p = 0.009$), indicating that the NAI group had generally higher motor imitation fidelity scores than the ASD group. Similarly, our ANCOVA results showed that a significant group difference remained in SRS-2 scores ($F = 25.76$, $p < 0.001$) and CAMI scores ($F = 5.53$, $p = 0.02$) even after controlling for demographic variables including age, sex, and handedness. Interestingly, we observed a significant effect of sex on the CAMI scores across the entire sample with males scoring higher than females ($F = 4.33$, $p = 0.04$). No significant group and sex interaction ($F = 0.04$, $p = 0.85$) was found, indicating that the influence of sex on CAMI scores was consistent across both groups.

3.2. Neural correlates of motor observation and imitation

During motor observation, significant activation (Fig. 2; FDR corrected $p < 0.05$) was found in occipital, temporal, and prefrontal cortex compared with the resting state. Bilateral regions throughout the visual cortex ($t > 5.74$, Cohen's D > 0.66, FDR corrected $p < 0.001$), including the occipital lobe, were highly engaged during observation. In temporal cortex, the superior temporal gyrus (STG, $t = 6.05$, Cohen's D = 0.69, FDR corrected $p = 1 \times 10^{-6}$), medial temporal gyrus (MTG, $t = 5.53$, Cohen's D = 0.63, FDR corrected $p = 0.006$), and fusiform gyrus (FFG, $t = 5.10$, Cohen's D = 0.58, FDR corrected $p = 0.003$) were also strongly recruited. Bilateral inferior frontal gyrus (IFG, $t = 4.77$, Cohen's D = 0.58, FDR corrected $p = 0.003$) and inferior parietal lobe (IPL, $t = 4.62$, Cohen's D = 0.53, FDR corrected $p = 0.002$) were also strongly activated during observation compared with the resting state.

During motor imitation, additional regions of activation extended beyond above regions (i.e., STG, MTG, FFG, and IFG) and included key motor-related areas (Fig. 2; FDR corrected $p < 0.05$). The primary motor cortex (M1, $t = 3.18$, Cohen's D = 0.40, FDR corrected $p = 0.009$), premotor cortex (PMC, $t = 3.19$, Cohen's D = 0.40, FDR corrected $p = 0.02$), and supplementary motor area (SMA, $t = 2.91$, Cohen's D = 0.37, FDR corrected $p = 0.02$) showed significant engagement during motor imitation. Additionally, the frontal eye field (FEF, $t = 2.93$, Cohen's

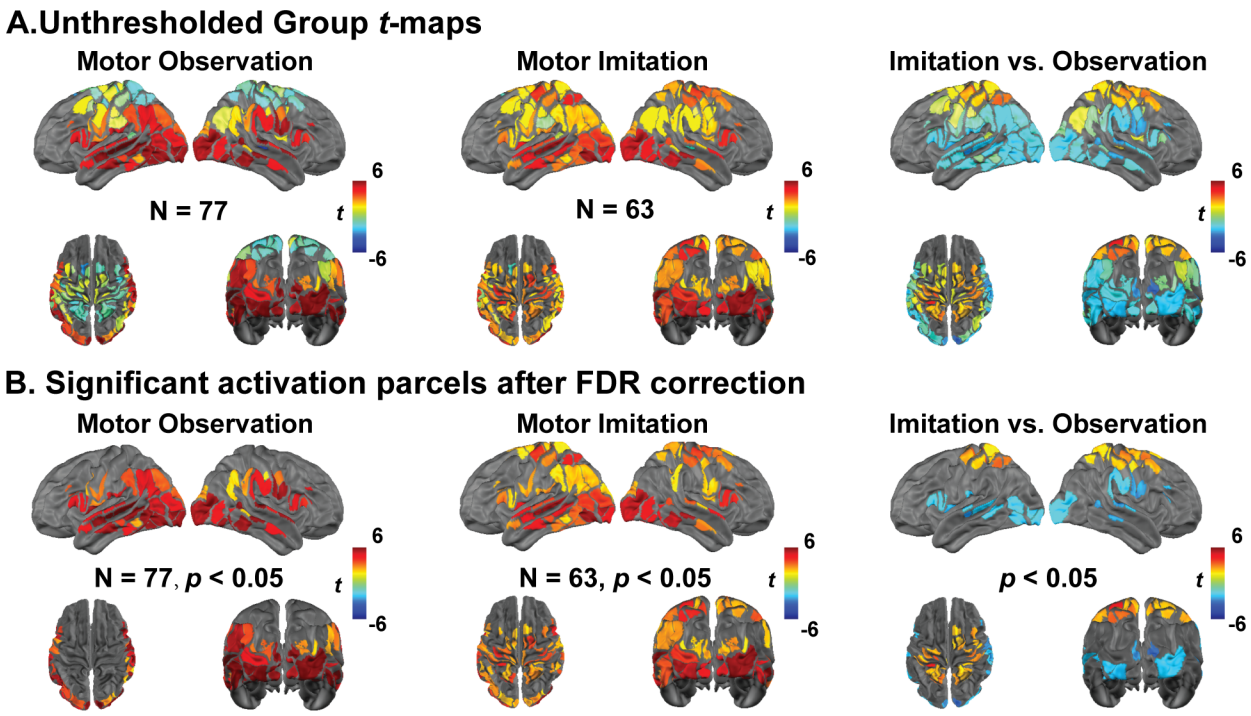

Fig. 2. Neural correlates of observation and imitation. (A) Group-level t-maps for motor observation (n = 77), motor imitation (n = 63), and their contrast (imitation vs. observation). (B) FDR-corrected t-maps highlighting statistically significant regions with false discovery rate correction (FDR corrected $p < 0.05$) applied to account for multiple comparisons.

D = 0.37, FDR corrected p = 0.01) and superior parietal lobules (SPL, t = 3.39, Cohen's D = 0.43, FDR corrected p = 0.01) exhibited significant activations compared with the resting state.

Conjunction analyses of overlapping activation for imitation and observation task states revealed activation in MNS regions, including IPL, STG, and IFG, as well as in bilateral occipital lobe, FFG, and MTG regions (Fig. 3). Despite these similarities, consistent with above, direct contrast of imitation versus observation task states revealed significant activation (Fig. 2B; FDR corrected $p < 0.05$) in motor/premotor regions, including bilateral M1 (t = 2.91, Cohen's D = 0.49, FDR corrected p = 0.02), PMC (t = 2.50, Cohen's D = 0.42, FDR corrected p = 0.03), and SMA (t = 2.43, Cohen's D = 0.41, FDR corrected p = 0.03; Fig. 4, imitation > observation). In contrast, other regions exhibited significant activation for observation > imitation (Fig. 2B, FDR corrected $p < 0.05$), principally in posterior cortical regions: occipital and temporal cortex, including bilateral visual cortex (t = 2.48, Cohen's D = 0.41, FDR corrected p = 0.03), STG (t = 2.73, Cohen's D = 0.45, FDR corrected p = 0.02), and MTG (t = 2.48, Cohen's D = 0.40, FDR corrected p = 0.03). Additionally, IFG activation was also observed (t = 2.31, Cohen's D = 0.38, FDR corrected p = 0.04; Fig. 5, observation > imitation). These results revealed that motor imitation strongly activated motor-related regions, including M1, SMA, PMC, and parietal areas (Supplementary Fig. S2), which were inactive during observation. In contrast, observation primarily engaged action understanding and perceptual processing brain regions (Supplementary Fig. S3), with greater activation in the left IFG and right temporal parietal junction (TPJ), which remained inactive during the imitation task. This highlights the brain regions for analyzing rather than executing movement in the context of motor imitation. Notably, compared with observing, imitating led to significantly greater activation in extended MNS areas, including M1 and SMA (Supplementary Fig. S4B, C). To further investigate the observed brain activations from a functional network perspective, we quantified the number of cortical parcels activated within each network for each task (Supplementary Fig. S5). Most brain networks were dynamically engaged during motor observation and imitation tasks. The dorsal attention network and the somatosensory hand network (t = 2.63, Cohen's D = 0.45, FDR corrected p = 0.02) exhibited larger involvement during imitation than during observation (Supplementary Figs. S5D and S6). In contrast, the visual (t = 1.86, Cohen's D = 0.31, FDR corrected p = 0.04) and ventral attention network (VAN, t = 2.39, Cohen's D = 0.39, FDR corrected p = 0.03) exhibited greater recruitment during observation than during imitation (Supplementary Figs. S5D and S6). Overall, these results support our

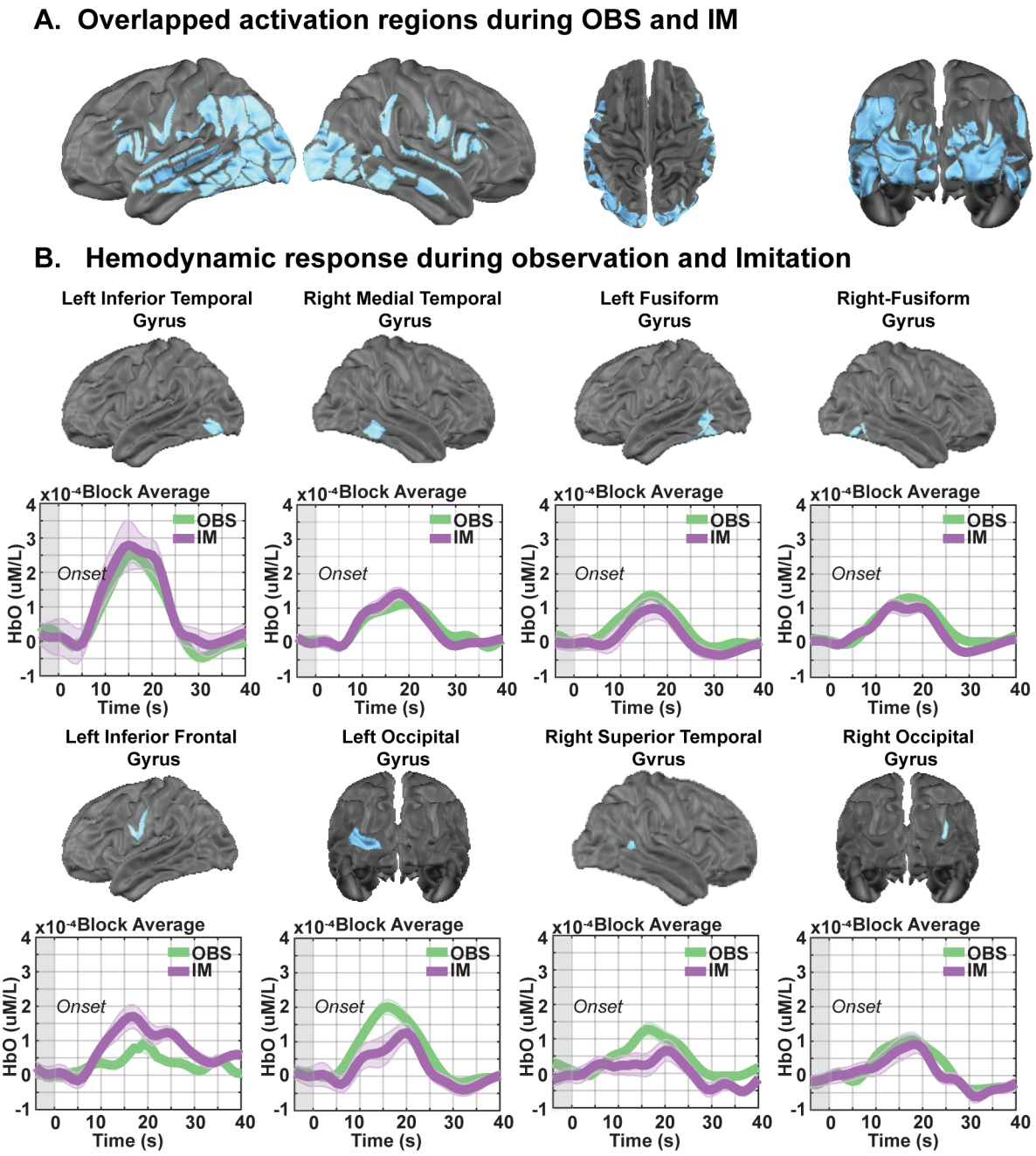

Fig. 3. Brain regions exhibiting significant responses to both motor observation and imitation. (A) Brain regions with overlapping significant activation (FDR corrected $p < 0.05$) identified through conjunction analysis. (B) Temporal profiles of the HbO (oxygenated hemoglobin) hemodynamic response for each task, with shaded areas indicating the standard error of the mean across participants. Time courses include a 5-second pre-stimulus baseline period (–5 to 0 seconds), with stimulus onset at 0 seconds.

hypothesis that both observation and imitation engage the MNS, with imitation showing stronger activation in extended MNS regions, including M1 and SMA. Additionally, as predicted, DAN showed greater activation during imitation, while VAN was more engaged during observation, confirming distinct network dynamics between the two tasks.

To ensure that the primary findings were not disproportionately influenced by the ASD subgroup, we conducted a follow-up group-level analysis restricted to neurotypical (NAI) participants only (N = 64 for motor observation, N = 50 for motor imitation). The unthresholded t-maps for motor observation, imitation, and the imitation-versus-observation contrast were consistent with those obtained in the full sample (N = 77 and N = 63, respectively; Supplementary Fig. S7A, B). Consistent bilateral activations were observed in premotor and parietal regions for both motor tasks, with enhanced

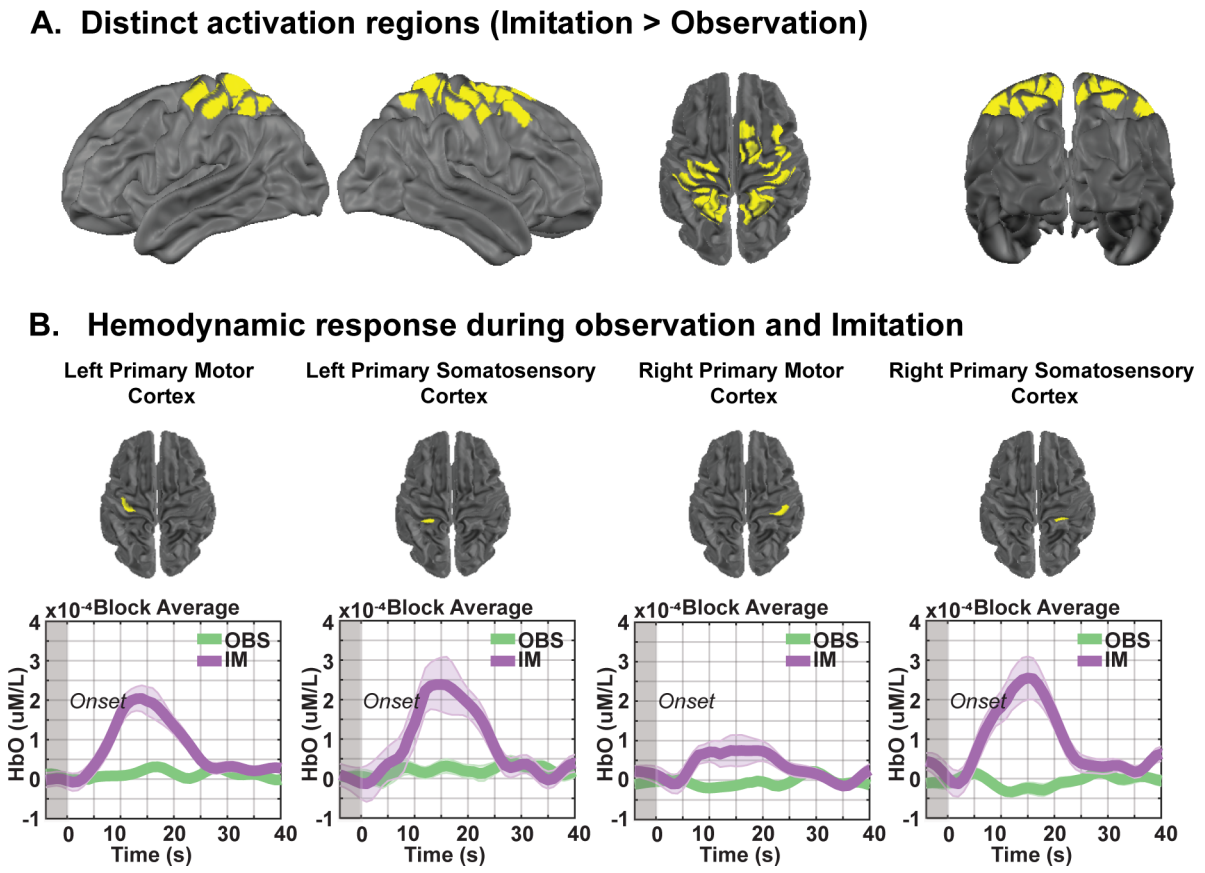

Fig. 4. Brain regions exhibiting significantly greater responses during motor imitation than during motor observation. (A) Brain regions exhibit significantly greater activation during motor imitation than during motor observation task. (B) Temporal profiles of the HbO (oxygenated hemoglobin) hemodynamic response for each task, with shaded areas representing the standard error of the mean across participants. Time courses include a 5-second pre-stimulus baseline period (–5 to 0 seconds), with stimulus onset at 0 seconds.

motor–parietal engagement during imitation relative to observation. Although the NAI-only maps exhibited slightly reduced spatial extent and lower peak t-values, as expected from the smaller sample size, the qualitative spatial patterns were preserved. These results support our rationale for collapsing across diagnostic groups in the main analyses: while the ASD subgroup was too small to support separate statistical testing, it contributed valuable behavioral variability without driving group-level neural activation patterns.

3.3. Associations with SRS-2

During the observation task, analysis revealed a significant positive correlation between SRS-2 T-scores and brain activation in the right SPL (Fig. 6A; r = 0.46, $p = 3.4 \times 10^{-5}$, FDR-corrected p = 0.007), such that individuals with higher autistic traits exhibited greater activation in the r-SPL during motor observation. Our multiple regression model, including SRS and demographic variables (i.e., age, sex, and handedness; Supplementary Table S2), predicted the brain region of r-SPL ($F(70) = 5.18$, R^2 = 0.24, adjusted R^2 = 0.19, $p < 0.001$). Additionally, among these predictors, SRS-2 scores significantly predicted the activation of right SPL (i.e., β = 0.43, t = 3.94, $p < 0.001$), while demographic variables did not (i.e., age: β = -0.10, t = 0.94, p = 0.34; sex: β = 0.15, t = 1.36, $p < 0.18$; and handedness: β = -0.03, t = 0.25, p = 0.80; Supplementary Table S2).

We found additional regional associations that were sub-threshold for significance and are presenting them as hypothesis-generating results for future studies that may be more strongly powered to test these effects. Specifically, we observed strong (but not passing FDR correction) positive correlations between SRS-2 T-scores and brain activation in the left IPL (r = 0.24, p = 0.045) and bilateral SMA (left SMA: r = 0.25, p = 0.03; right SMA: r = 0.28, p = 0.01) during the observation task. Moreover, analysis revealed that activation magnitudes in the bilateral occipital lobe (left occipital lobe: r = -0.31, p = 0.009; right occipital lobe: r = -0.24, p = 0.04) exhibited a negative correlation with SRS-2 scores (Fig. 6A). The

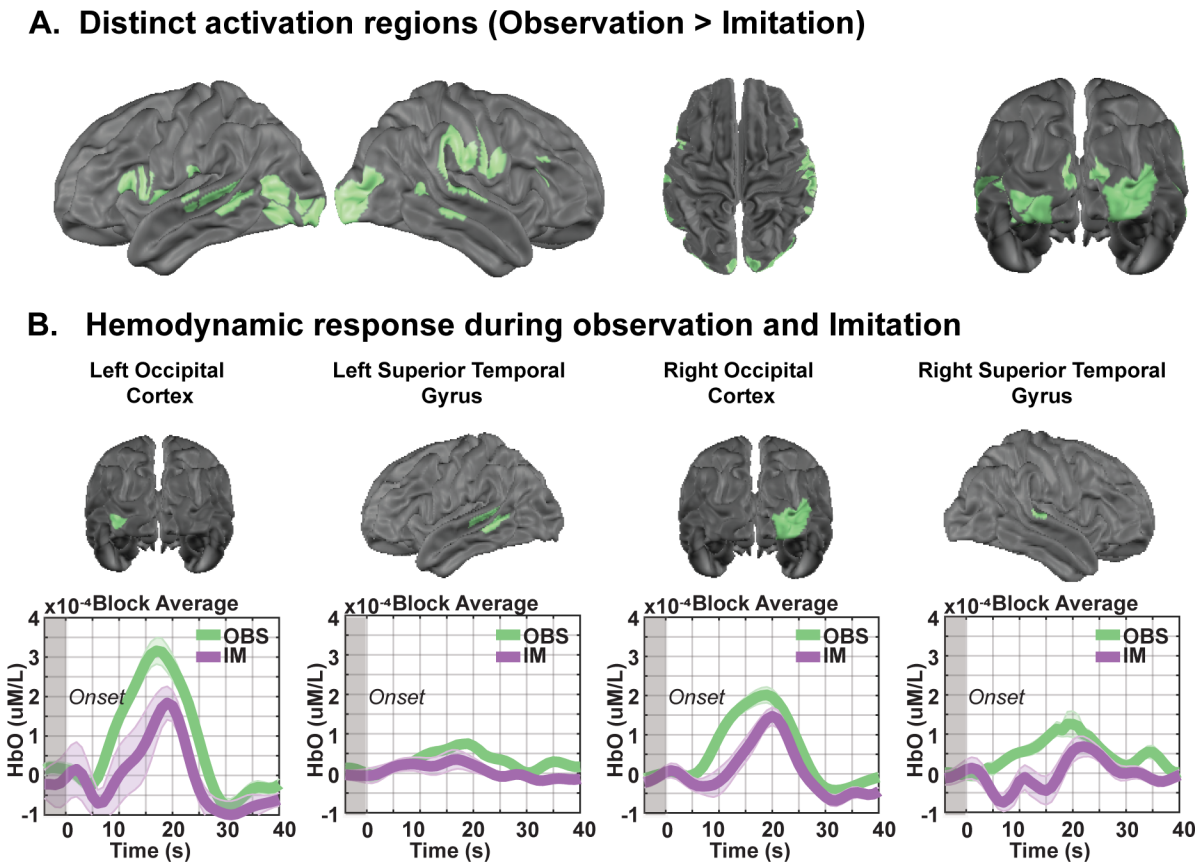

Fig. 5. Brain regions exhibiting significantly greater responses during motor observation than during motor imitation. (A) Brain regions exhibit significantly greater activation during motor observation than during motor imitation. (B) Temporal profiles of the HbO (oxygenated hemoglobin) hemodynamic response for each task, with shaded areas representing the standard error of the mean across participants. Time courses include a 5-second pre-stimulus baseline period (–5 to 0 seconds), with stimulus onset at 0 seconds.

regression model significantly predicted the brain activation in the right IPL ($F(70) = 5.18$, $R^2 = 0.24$, adjusted $R^2 = 0.19$, $p < 0.001$) and right occipital lobe ($F(70) = 6.42$, $R^2 = 0.28$, adjusted $R^2 = 0.24$, $p < 0.001$). Additionally, SRS-2 scores were the primary predictor for the brain activation prediction (right IPL: $\beta = 0.433$, $t = 3.94$, $p < 0.001$; right occipital lobe: $\beta = -0.40$, $t = 3.75$, $p < 0.001$) while controlling for demographic variables (i.e., age, sex, and handedness). However, after including demographic variables, the overall model did not reach statistical significance in other brain regions, such as the bilateral SMA (right SMA: $F(70) = 1.72$, $R^2 = 0.09$, adjusted $R^2 = 0.04$, $p = 0.16$; left SMA: $F(70) = 2.315$, $R^2 = 0.12$, adjusted $R^2 = 0.07$, $p = 0.07$), left IPL ($F(70) = 1.06$, $R^2 = 0.06$, adjusted $R^2 = 0.003$, $p = 0.39$), and left occipital lobe ($F(70) = 2.09$, $R^2 = 0.11$, adjusted $R^2 = 0.06$, $p = 0.09$). Nonetheless, SRS-2 still exhibited significant predictive power in the right SMA ($\beta = 0.29$, $t = 2.40$, $p = 0.02$) and left occipital lobe ($\beta = -0.32$, $t = 2.66$, $p = 0.01$). Additionally, we found a sex effect contribution ($\beta = -0.28$, $t = 2.60$, $p = 0.01$) to prediction of brain activation in the right occipital lobe along with SRS-2 scores.

During the imitation task, analysis revealed a negative correlation between SRS-2 T-scores and brain activation in the left subcentral gyrus (Fig. 6B; $r = -0.30$, $p = 0.03$). Multiple regression results indicated that the model explained variance in the left subcentral gyrus ($F(53) = 3.33$, $R^2 = 0.21$, adjusted $R^2 = 0.15$, $p = 0.02$). Similarly, the SRS-2 remained the significant predictor ($\beta = -0.38$, $t = 2.857$, $p = 0.006$), and sex also exhibited prediction power ($\beta = -0.36$, $t = 2.68$, $p < 0.01$), whereas age ($\beta = 0.10$, $t = 0.81$, $p = 0.43$) and handedness ($\beta = -0.10$, $t = 0.77$, $p = 0.45$) did not contribute significantly to the model. These findings suggest that individuals with higher autistic traits may exhibit diminished brain responses in the left subcentral gyrus during motor imitation tasks, though these correlations did not survive FDR correction.

Our hypothesis-driven analyses focusing on the mirror neuron system (MNS) revealed negative correlations between SRS-2 T-scores and activation in MNS-related regions, though these did not survive FDR correction. This finding suggests that individuals with elevated autistic traits may exhibit lower activity in MNS areas during

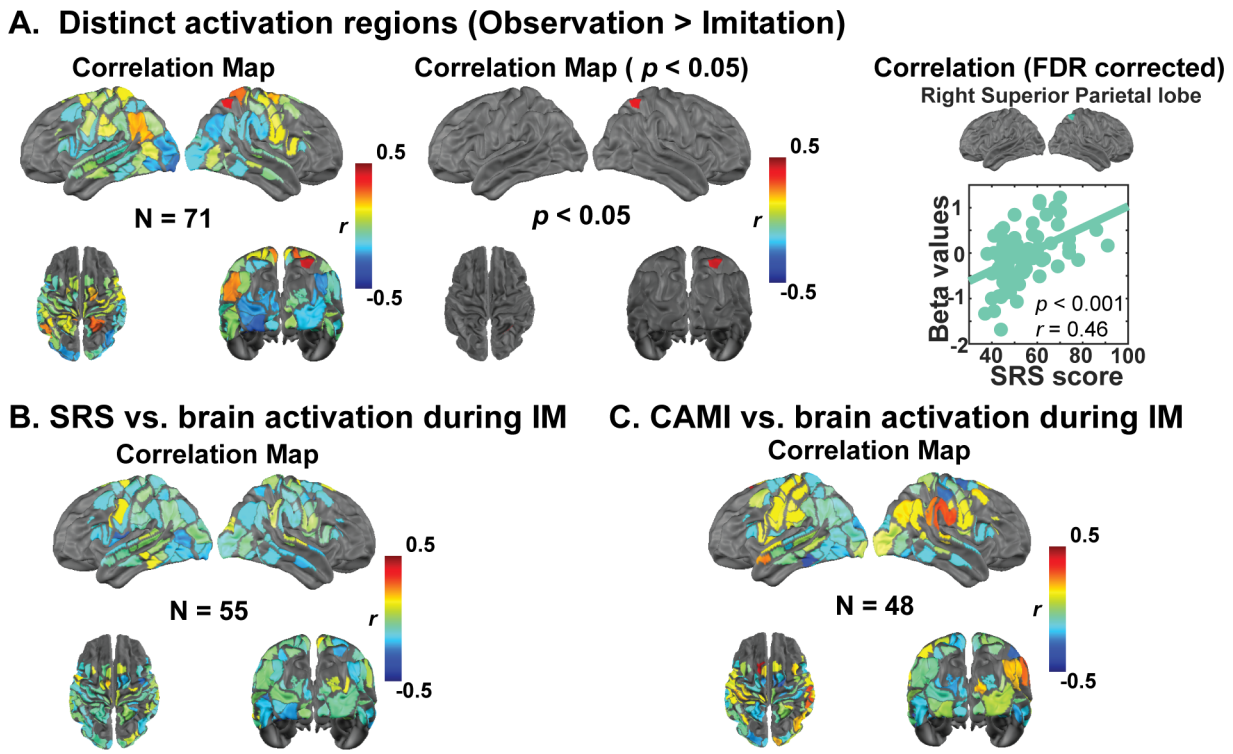

Fig. 6. Brain–behavioral association between SRS-2 t-scores and brain activation. (A) **(i)** Correlation map of brain activation during motor observation with SRS-2 in 71 participants, **(ii)** the brain regions which correlation $p < 0.05$, and **(iii)** the correlation passed the FDR correction ($r = 0.472$, and FDR corrected $p = 0.007$, and). (B) Correlation map of brain activation during motor imitation with SRS-2 in 55 participants. (C) Brain–behavioral association between CAMI and brain activation during motor imitation task for 48 participants.

social tasks. No significant correlations were found between SRS-2 scores and activation in the dorsal or ventral attention networks (DAN or VAN) during imitation.

3.4. Associations with CAMI

No brain activity correlations with CAMI scores remained statistically significant after applying FDR correction (Fig. 6C). We are presenting sub-FDR-threshold results as hypothesis-generating information for future studies. First, positive correlations were observed in left FEF ($r = 0.43$, $p = 0.002$; Supplementary Table S3) and right IPL ($r = 0.31$, $p = 0.03$, within MNS). Conversely, negative correlations were identified in right M1 ($r = -0.29$, $p = 0.04$, within MNS) and left FFG ($r = 0.34$, $p = 0.02$). Separate multiple regression models were conducted per brain region of interest, with CAMI scores as the predictor and age, sex, and handedness as the control variables. The model predicted brain activation in the left FEF ($F(46) = 4.96$, $R^2 = 0.32$, adjusted $R^2 = 0.26$, $p = 0.002$) and right IPL ($F(46) = 2.83$, $R^2 = 0.21$, adjusted $R^2 = 0.14$, $p = 0.04$). Among these predictors, the CAMI scores predicted the brain variance in left FEF ($\beta = 0.439$, $t = 3.30$, $p = 0.002$) and right IPL ($\beta = 0.37$, $t = 2.58$, $p = 0.01$). Similarly, the CAMI score independently contributed to predicting activation in right M1 ($\beta = -0.31$, $t = 2.10$, $p = 0.04$) and left FFG ($\beta = -0.31$, $t = 2.13$, $p = 0.04$). The model with demographic variables did not explain the brain activation significantly in right M1 ($F(46) = 2.28$, $R^2 = 0.18$, adjusted $R^2 = 0.10$, $p = 0.13$) and left FFG ($F(46) = 1.90$, $R^2 = 0.21$, adjusted $R^2 = 0.14$, $p = 0.07$). Interestingly, we also found age contributed to explain the variance of brain activation in the left FEF along with the primary factor (i.e., CAMI score; $\beta = -0.39$, $t = 2.97$, $p = 0.005$). Additionally, handedness predicted the correlation of brain activity in the right IPL with CAMI scores ($\beta = -0.32$, $t = 2.19$, $p = 0.03$).

4. DISCUSSION

This study investigated brain activation underlying naturalistic motor observation and imitation under more naturalistic conditions than possible using fMRI. Our findings revealed both shared and task-specific brain activation patterns for observation and imitation. Consistent with our hypothesis, we found that the core MNS regions, including the superior temporal gyrus (STG), inferior parietal lobule (IPL), and inferior frontal gyrus (IFG), were engaged during both tasks, with imitation evoking significantly greater activation in the primary

motor cortex (M1), premotor cortex (PMC), and supplementary motor area (SMA), underscoring their involvement in coordinating and executing motor imitative actions. Additionally, as we hypothesized, regions within the DAN and VAN were engaged during both tasks, with stronger activation in key DAN and MNS regions during motor imitation. In contrast, the temporoparietal junction (TPJ) was engaged during observation but remained less active during imitation. Contrary to our hypothesis, higher autistic traits (SRS-2 scores) were associated with increased activation in the right SPL during observation and decreased activation in the left subcentral gyrus during imitation, and CAMI scores showed only trend-level associations with brain activity. These findings provide valuable insights into how brain activation variability in specific brain regions contributes to motor imitation deficits and their association with autistic traits.

4.1. Neural activation patterns during motor observation

During motor observation (Figs. 2 and 5; Supplementary Fig. S3), significant activations were observed in the STG, IPL, IFG, and TPJ—regions closely associated with the MNS and VAN, and known to facilitate the processing of observed actions (Cattaneo & Rizzolatti, 2009; Chan & Han, 2020; Iacoboni & Dapretto, 2006). The STG, particularly the posterior STG, exhibited strong activity, which aligns with its role in mapping observed actions onto internal neural spatial–temporal representations, as it is usually considered as a visual input of MNS (Cattaneo & Rizzolatti, 2009; Iacoboni & Dapretto, 2006; Marsh & Hamilton, 2011; Su et al., 2020; Tylen et al., 2012). The right TPJ, part of the VAN, was strongly activated during motor observation but not during motor imitation. This aligns with its role in stimulus-driven attention and social perception, particularly when the participant observes the actor's movements without the demands of imitation (Sowden & Catmur, 2015). Additionally, the right TPJ is crucial for understanding others' actions, intentions, and goals, making it highly relevant for observational learning (Mizuguchi et al., 2016; Sowden & Catmur, 2015). However, during imitation, its activity diminishes as the cognitive focus shifts from action interpretation to direct motor execution. This transition from motor observation to first-person motor mapping is supported by the involvement of the IFG and IPL, key regions of the MNS, which facilitate action understanding and execution (Iacoboni et al., 2005; Rizzolatti & Fabbri-Destro, 2008). The IFG, particularly, has been shown to play a role in action imitation and motor planning, while the IPL contributes to sensorimotor integration with spatial–temporal representations of motor intention (Kilner et al., 2006). Together, these areas shift the neural representation from a passive observational stance to active, embodied execution during imitation (Chan & Han, 2020; Iacoboni et al., 2005; Rizzolatti & Fabbri-Destro, 2008).

4.2. Neural activation patterns during motor imitation

Motor imitation elicited significantly stronger activations in primary motor cortex (M1), supplementary motor area (SMA), dorsal premotor cortex (PMC), and the intraparietal sulcus (IPS) compared with motor observation (Figs. 2 and 4; Supplementary Fig. S3). The SMA and PMC play key roles in motor planning and movement coordination (Nachev et al., 2007; Sadato et al., 1997), explaining their enhanced activity when participants transitioned from passively observing movements to actively reproducing them. Additionally, the posterior parietal cortex, particularly the IPS, plays a crucial role in visual–motor integration by combining visual and spatial information necessary to planning and executing goal-directed movements (Iacoboni, 2006). A direct contrast between imitation and observation revealed additional recruitment from posterior temporal–parietal regions (i.e., STG, IPL) and frontal–motor regions (i.e., M1, SMA, PMC, IFG). This additional neural recruitment is expected, as imitation requires additional motor control mechanisms beyond those used for passive action recognition (Iacoboni et al., 1999). The increased activation of the SMA and PMC during motor imitation (compared with observation) supports their well-established role in internally generating motor sequences based on observed actions.

4.3. Shared neural patterns between observation and imitation

Our findings also reveal that there is a large degree of shared brain activation pattern between motor imitation and observation, particularly within the MNS (Fig. 3; Supplementary Fig. S4). Both tasks recruit a shared network of brain regions involved in perception and motor planning, including the bilateral occipital lobe, STG, MTG, FFG, IFG, and IPL (Fig. 3). The concurrent activation of these areas suggests that the brain processes observed movements in a way that not only supports action understanding but also primes the motor system for potential execution. This functional overlap underscores the role of these regions in action encoding, reinforcing the idea that motor imitation and observation rely on a common neural substrate that bridges perception and action.

4.4. Task-specific neural profiles for observation and imitation

While our findings align with the literature on the neural basis of imitation as stated above, they also provide new insights into the task-specific neural profiles during the gross motor observation and imitation as well as the evidence of a structured neural progression from posterior sensory regions to anterior motor areas (Freedman & Ibos, 2018). This highlights the hierarchical organization of motor learning, wherein initial sensory-driven processing in temporal–parietal regions is followed by predictive coding and motor planning in SMA and PMC (Nachev et al., 2007; Orban et al., 2021). Additionally, the differential activation of the TPJ during observation versus imitation suggests additional neural recruitment from externally driven attention toward internally guided motor execution (Krall et al., 2015; Sowden & Catmur, 2015). These results suggest that imitation engages a specialized motor planning mechanism beyond passive observation, emphasizing the STG, SMA, and PMC as critical hubs for transforming visual input into executable motor commands (Iacoboni et al., 2005; Sadato et al., 1997; Su et al., 2023).

Beyond the MNS, our findings highlight the differential engagement of the VAN and DAN across tasks. Our results reveal that there was greater VAN activation during observation than imitation (Supplementary Figs. S5 and S6), supporting its role in detecting and processing salient external stimuli (Corbetta & Shulman, 2002; He et al., 2007; Nardo et al., 2011; Vossel et al., 2014). Additionally, the heightened activation of right TPJ (Supplementary Fig. S3) suggests that passive observation of human actions relies heavily on stimulus-driven attention and social cue processing (Mizuguchi et al., 2016; Sowden & Catmur, 2015). Conversely, the DAN (including IPS and frontal eye fields, FEF) was more engaged during imitation than during observation, which aligns with its function in goal-directed attention and action planning (Supplementary Fig. S6). The increased IPS activity during imitation might indicate that spatial and motor attention play a crucial role in translating visual input into coordinated movements. This contrast between VAN and DAN activation aligns with previous findings that observation primarily involves passive stimulus-driven processing, whereas imitation requires active attentional control and motor planning.

4.5. Brain–behavior association between imitation fidelity and brain activation

The analysis of brain–behavior correlations between brain activation and CAMI scores revealed associations in MNS regions implicated in motor planning and execution. Positive correlations were observed in right parietal and left superior frontal gyrus, suggesting that greater motor imitation fidelity (i.e., higher CAMI scores) is linked to enhanced activation in these areas. Interestingly, we found a negative correlation in the right primary motor cortex and left middle temporal gyrus, which does not align with the hypothesis that stronger motor system engagement supports better imitation performance. However, the reduced activation in the right M1 could reflect greater efficiency in motor processing, where less activation may indicate that the brain is optimizing motor control without needing additional cortical resources (Mishra et al., 2024; Picard et al., 2013). An fMRI study found a positive correlation in the primary motor cortex with participants' motor performance (Aridan & Mukamel, 2016). Another study found inferior parietal lobe (IPL; also implicated as part of the MNS) activity was negatively correlated with imitation accuracy (Kruger et al., 2014). Moreover, extant literature states that reduced activation in the core MNS regions may be associated with difficulties in motor adaptability (Iacoboni et al., 2005; Marsh & Hamilton, 2011; Villalobos et al., 2005). These findings provide insight into how deficits in neural regions critical for motor control and imitation may contribute to reduced imitation fidelity in autistic individuals.

4.6. Brain–behavior association between autistic trait and brain activation

The relationship between brain activation and social responsiveness was further investigated for both motor observation and imitation. Positive correlations between SRS-2 T-scores and brain activation were observed in regions such as the right angular gyrus (r-AG) and left secondary visual cortex (l-SVC), particularly during observation. Although these correlations did not reach statistical significance during motor imitation, they provide preliminary evidence that impaired brain function in regions involved in action understanding and social cognition may underlie the social difficulties observed in ASD. Interestingly, our results show a positive correlation between SRS-2 T-scores and brain activation in the right parietal lobe. This result diverges from our original hypothesis, which posited that brain response strength within the MNS during observation and imitation would be negatively correlated with dimensional measures of autistic traits. Instead of a reduced brain activation linked to higher autistic traits, our data indicated an enhanced reliance on the right parietal lobe in individuals with stronger autistic traits. This finding may indicate that individuals with higher autistic traits rely more heavily on this region to process and understand observed actions or

social cues, potentially compensating for challenges in other aspects of social interaction (Kinard et al., 2020).

4.7. Limitations

While this study provides valuable insights into neural correlates of motor observation and imitation and their association with autistic traits, several limitations should be addressed in future research. First, the relatively small sample size of the ASD group limits the generalizability of the findings in autistic individuals. Rather, we used a dimensional approach, incorporating ASD samples to represent a broad range of behavioral traits and to conduct brain-behavior associations during motor observation and imitation. Future studies with larger and more diverse populations are needed to confirm and extend these results. Second, although HD-DOT offers significant advantages over traditional neuroimaging methods, its field of view is less extensive than that of fMRI, which limits sensitivity to neural activity in deeper regions such as cerebellum and sub-cortical regions previously implicated in ASD functional neuroimaging studies (Cerliani et al., 2015; Laidi et al., 2017). Third, we did not use eye tracking to monitor eye gaze and visual attention throughout the experiment. Instead, participants were instructed to focus their attention on the screen, and they were continuously visually monitored for attention and imitation performance by the laboratory member conducting the study. Such simultaneous collection of eye gaze with neuroimaging and 3D motion tracking will provide a powerful strategy for future studies to more fully investigate the role of visual attention on motor output. Fourth, in this study, data loss from the initial 100 participants occurred due to independent exclusions across different data types, including HD-DOT quality (i.e., 22%), missing SRS-2 scores (i.e., 9%), and CAMI recording (i.e., 11%) issues. These exclusions did not systematically affect the same participants across modalities or groups. Additionally, to avoid potential practice effects associated with repeated task, brain–behavior analyses involving CAMI were further restricted to participants whose HD-DOT data met quality thresholds during the first imitation run and CAMI recording video. This resulted in a final subset of 48 participants (including both ASD and NAI) for the CAMI–brain association analysis. While this yield may seem modest, it reflects the combined demands of motion-sensitive neuroimaging, behavioral motion tracking, and our conservative data quality criteria. Finally, although the current study focused on adults, future studies that focus on how brain function supports naturalistic motor imitation throughout childhood development, including in children with and without autism, will be positioned to inform brain-region-targeted interventions and advance precision medicine. Those investigations will provide valuable insights into the developmental aspects of naturalistic motor imitation, shedding light on how these mechanisms may differ throughout the lifespan and how they may contribute to the social and motor challenges observed in children with ASD.

5. CONCLUSION

In this study, we used simultaneous HD-DOT functional neuroimaging with the CAMI method to investigate how brain function covaries with naturalistic motor observation and imitation. Consistent with our hypotheses based on prior fMRI studies under less naturalistic conditions, our findings revealed commonality of neural activation patterns for motor observation and imitation, principally within MNS regions. We also observed some clear distinctions in neural activation patterns between passive action observation and active motor imitation. Observation relies more on temporal–parietal regions (e.g., STG, IPL, TPJ) and the VAN, reflecting stimulus-driven processing of movement cues. In contrast, imitation engages prefrontal and motor regions (M1, SMA, PMC, IFG) and the DAN, highlighting the additional demands of motor planning and execution. The additional neural recruitment from posterior (sensory-driven) to anterior (motor-driven) cortical activation during imitation underscores the neural transformation from perception to action execution. Moreover, our brain–behavior analyses indicated that reduced MNS activation may be associated with higher autism-related traits and lower motor imitation fidelity. Overall, these findings highlight the neural correlates of action observation and execution, associated social reciprocity, and motor imitation fidelity. Finally, these studies lay an essential foundation for future investigations using simultaneous methods for naturalistic functional neuroimaging and quantitative CAMI that may be applied during early childhood screenings for ASD.

DATA AND CODE AVAILABILITY

The datasets generated and analyzed during the current study, as well as the analysis codes, are available from the corresponding author upon request. All fully de-identified data will also be available post-publication on the NIMH data archive (NDA) and the OXI (www.oxi.wustl.edu) data sharing site. Please contact the author for more information.

AUTHOR CONTRIBUTIONS

Conceptualization: A.T.E., S.H.M. Data collection: D.Y., T.G.G., C.M.S., S.R.M., K.T.K., E.D.D., S.M.P., E.S., A.S. Formal analyses: D.Y., T.G.G., A.T.E. Methodology: D.Y.,

C.P., R.R., D.C., A.D.S., M.B.N., B.T., R.V., N.M., S.H.M., A.T.E. Project administration: A.T.E., S.H.M. Resources: A.T.E., S.H.M. Software: A.T.E., S.H.M., B.T. Visualization: D.Y., A.T.E. Writing: D.Y., A.T.E. Funding acquisition: A.T.E., S.H.M. All authors read and approved the final manuscript.

DECLARATION OF COMPETING INTEREST

The authors declare that they have no competing interests related to this work.

ACKNOWLEDGMENTS

We would like to express our sincere gratitude to the participants for their valuable contributions to this study. This research was supported by grants from the National Institutes of Health (R01-MH12275101, R21-MH127501), the McDonnell Center for Systems Neuroscience, the Simons Foundation for Autism Research (SFARI), and the Eagles Autism Foundation. All study procedures were reviewed and approved by the Human Protections Office at the Washington University School of Medicine Institutional Review Boards. Written informed consent was obtained from all participants. Additionally, the individuals shown in the image in Figure 1 provided consent for the use of their photographs in publications.

SUPPLEMENTARY MATERIALS

Supplementary material for this article is available with the online version here: https://doi.org/10.1162/IMAG.a.153.

REFERENCES

Aridan, N., & Mukamel, R. (2016). Activity in primary motor cortex during action observation covaries with subsequent behavioral changes in execution. *Brain and Behavior*, *6*(11), e00550. https://doi.org/10.1002/brb3.550

Bhat, A. N. (2020). Is motor impairment in autism spectrum disorder distinct from developmental coordination disorder? A report from the SPARK study. *Physical Therapy*, *100*(4), 633–644. https://doi.org/10.1093/ptj/pzz190

Blanco, B., Lloyd-Fox, S., Begum-Ali, J., Pirazzoli, L., Goodwin, A., Mason, L., Pasco, G., Charman, T., Jones, E. J. H., & Johnson, M. H. (2023). Cortical responses to social stimuli in infants at elevated likelihood of ASD and/or ADHD: A prospective cross-condition fNIRS study. *Cortex*, *169*, 18–34. https://doi.org/10.1016/j.cortex.2023.07.010

Buccino, G., Vogt, S., Ritzl, A., Fink, G. R., Zilles, K., Freund, H. J., & Rizzolatti, G. (2004). Neural circuits underlying imitation learning of hand actions: An event-related fMRI study. *Neuron*, *42*(2), 323–334. https://doi.org/10.1016/s0896-6273(04)00181-3

Cattaneo, L., & Rizzolatti, G. (2009). The mirror neuron system. *Archives of Neurology*, *66*(5), 557–560. https://doi.org/10.1001/archneurol.2009.41

Celebi, S., Aydin, A. S., Temiz, T. T., & Arici, T. (2013). Gesture recognition using skeleton data with weighted dynamic time warping. *International Conference on Computer Vision Theory and Applications*, *1*, 620–625. https://doi.org/10.5220/0004217606200625

Cerliani, L., Mennes, M., Thomas, R. M., Di Martino, A., Thioux, M., & Keysers, C. (2015). Increased functional connectivity between subcortical and cortical resting-state networks in autism spectrum disorder. *JAMA Psychiatry*, *72*(8), 767–777. https://doi.org/10.1001/jamapsychiatry.2015.0101

Chaminade, T., Meltzoff, A. N., & Decety, J. (2005). An fMRI study of imitation: Action representation and body schema. *Neuropsychologia*, *43*(1), 115–127. https://doi.org/10.1016/j.neuropsychologia.2004.04.026

Chan, M. M. Y., & Han, Y. M. Y. (2020). Differential mirror neuron system (MNS) activation during action observation with and without social-emotional components in autism: A meta-analysis of neuroimaging studies. *Molecular Autism*, *11*(1), 72. https://doi.org/10.1186/s13229-020-00374-x

Chitnis, D., Cooper, R. J., Dempsey, L., Powell, S., Quaggia, S., Highton, D., Elwell, C., Hebden, J. C., & Everdell, N. L. (2016). Functional imaging of the human brain using a modular, fibre-less, high-density diffuse optical tomography system. *Biomed Opt Express*, *7*(10), 4275–4288. https://doi.org/10.1364/BOE.7.004275

Collins-Jones, L. H., Gossé, L. K., Blanco, B., Bulgarelli, C., Siddiqui, M., Vidal-Rosas, E. E., Duobaitė, N., Nixon-Hill, R. W., Smith, G., Skipper, J., Sargent, T., Powell, S., Everdell, N. L., Jones, E. J. H., & Cooper, R. J. (2024). Whole-head high-density diffuse optical tomography to map infant audio-visual responses to social and non-social stimuli. *Imaging Neuroscience*, *2*, 1–19. https://doi.org/10.1162/imag_a_00244

Constantino, J. N., Davis, S. A., Todd, R. D., Schindler, M. K., Gross, M. M., Brophy, S. L., Metzger, L. M., Shoushtari, C. S., Splinter, R., & Reich, W. (2003). Validation of a brief quantitative measure of autistic traits: Comparison of the social responsiveness scale with the autism diagnostic interview-revised. *Journal of Autism and Developmental Disorders*, *33*(4), 427–433. https://doi.org/10.1023/a:1025014929212

Corbetta, M., Patel, G., & Shulman, G. L. (2008). The reorienting system of the human brain: From environment to theory of mind. *Neuron*, *58*(3), 306–324. https://doi.org/10.1016/j.neuron.2008.04.017

Corbetta, M., & Shulman, G. L. (2002). Control of goal-directed and stimulus-driven attention in the brain. *Nature Reviews Neuroscience*, *3*(3), 201–215. https://doi.org/10.1038/nrn755

Crone, E. A., Poldrack, R. A., & Durston, S. (2010). Challenges and methods in developmental neuroimaging. *Human Brain Mapping*, *31*(6), 835–837. https://doi.org/10.1002/hbm.21053

Dapretto, M., Davies, M. S., Pfeifer, J. H., Scott, A. A., Sigman, M., Bookheimer, S. Y., & Iacoboni, M. (2006). Understanding emotions in others: Mirror neuron dysfunction in children with autism spectrum disorders. *Nat Neurosci*, *9*(1), 28–30. https://doi.org/10.1038/nn1611

Datko, M., Pineda, J. A., & Müller, R.-A. (2018). Positive effects of neurofeedback on autism symptoms correlate with brain activation during imitation and observation. *European Journal of Neuroscience*, *47*(6), 579–591. https://doi.org/10.1111/ejn.13551

Dushanova, J., & Donoghue, J. (2010). Neurons in primary motor cortex engaged during action observation. *Eur J Neurosci*, *31*(2), 386–398. https://doi.org/10.1111/j.1460-9568.2009.07067.x

Eggebrecht, A. T., Ferradal, S. L., Robichaux-Viehoever, A., Hassanpour, M. S., Dehghani, H., Snyder, A. Z., Hershey, T., & Culver, J. P. (2014). Mapping distributed brain function and networks with diffuse optical tomography. *NATURE PHOTONICS*, *8*(6), 448–454. https://doi.org/10.1038/nphoton.2014.107

Eggebrecht, A. T., White, B. R., Ferradal, S. L., Chen, C. X., Zhan, Y. X., Snyder, A. Z., Dehghani, H., & Culver, J. P. (2012). A quantitative spatial comparison of high-density diffuse optical tomography and fMRI cortical mapping. *NeuroImage*, *61*(4), 1120–1128. https://doi.org/10.1016/j.neuroimage.2012.01.124

Falck-Ytter, T., Gredebäck, G., & von Hofsten, C. (2006). Infants predict other people's action goals. *Nature Neuroscience*, *9*(7), 878–879. https://doi.org/10.1038/nn1729

Fan, W., Trobaugh, J. W., Zhang, C., Yang, D., Culver, J. P., & Eggebrecht, A. T. (2025). Fundamental effects of array density and modulation frequency on image quality of diffuse optical tomography. *Medical Physics*, *52*(2), 1045–1057. https://doi.org/10.1002/mp.17491

Ferradal, S. L., Eggebrecht, A. T., Hassanpour, M., Snyder, A. Z., & Culver, J. P. (2014). Atlas-based head modeling and spatial normalization for high-density diffuse optical tomography: Validation against fMRI. *NeuroImage*, *85*, 117–126. https://doi.org/10.1016/j.neuroimage.2013.03.069

Ferradal, S. L., Liao, S., Eggebrecht, A. T., Shimony, J. S., Inder, T. E., Culver, J. P., & Smyser, C. D. (2016). Functional Imaging of the Developing Brain at the Bedside Using Diffuse Optical Tomography. *CEREBRAL CORTEX*, *26*(4), 1558–1568. https://doi.org/10.1093/cercor/bhu320

Fishell, A. K., Arbelaez, A. M., Valdes, C. P., Burns-Yocum, T. M., Sherafati, A., Richter, E. J., Torres, M., Eggebrecht, A. T., Smyser, C. D., & Culver, J. P. (2020). Portable, field -based neuroimaging using high -density diffuse optical tomography. *NeuroImage*, *215*, Article 116541. https://doi.org/10.1016/j.neuroimage.2020.116541

Fishell, A. K., Burns-Yocum, T. M., Bergonzi, K. M., Eggebrecht, A. T., & Culver, J. P. (2019). Mapping brain function during naturalistic viewing using high-density diffuse optical tomography. *Scientific Reports*, *9*, 11115. https://doi.org/10.1038/s41598-019-45555-8

Freedman, D. J., & Ibos, G. (2018). An Integrative Framework for Sensory, Motor, and Cognitive Functions of the Posterior Parietal Cortex. *Neuron*, *97*(6), 1219–1234. https://doi.org/10.1016/j.neuron.2018.01.044

Frijia, E. M., Billing, A., Lloyd-Fox, S., Vidal Rosas, E., Collins-Jones, L., Crespo-Llado, M. M., Amado, M. P., Austin, T., Edwards, A., Dunne, L., Smith, G., Nixon-Hill, R., Powell, S., Everdell, N. L., & Cooper, R. J. (2021). Functional imaging of the developing brain with wearable high-density diffuse optical tomography: A new benchmark for infant neuroimaging outside the scanner environment. *NeuroImage*, *225*, 117490. https://doi.org/10.1016/j.neuroimage.2020.117490

Fuentes, C. T., Mostofsky, S. H., & Bastian, A. J. (2011). No proprioceptive deficits in autism despite movement-related sensory and execution impairments. *J Autism Dev Disord*, *41*(10), 1352–1361. https://doi.org/10.1007/s10803-010-1161-1

Geurts, H. M., Verté, S., Oosterlaan, J., Oosterlaan, J., Roeyers, H., Roeyers, H., Sergeant, J. A., & Sergeant, J. A. (2004). How specific are executive functioning deficits in attention deficit hyperactivity disorder and autism? *Journal of Child Psychology and Psychiatry*, *45*(4), 836–854. https://doi.org/10.1111/j.1469-7610.2004.00276.x

Gordon, E. M., Laumann, T. O., Adeyemo, B., Huckins, J. F., Kelley, W. M., & Petersen, S. E. (2016). Generation and evaluation of a cortical area parcellation from resting-state correlations. *Cerebral Cortex*, *26*(1), 288–303. https://doi.org/10.1093/cercor/bhu239

Gregg, N. M., White, B. R., Zeff, B. W., Berger, A. J., & Culver, J. P. (2010). Brain specificity of diffuse optical imaging: Improvements from superficial signal regression and tomography. *Front Neuroenergetics*, *2*, 14. https://doi.org/10.3389/fnene.2010.00014

Habermehl, C., Holtze, S., Steinbrink, J., Koch, S. P., Obrig, H., Mehnert, J., & Schmitz, C. H. (2012). Somatosensory activation of two fingers can be discriminated with ultrahigh-density diffuse optical tomography. *NeuroImage*, *59*(4), 3201–3211. https://doi.org/10.1016/j.neuroimage.2011.11.062

Hassanpour, M. S., Eggebrecht, A. T., Peelle, J. E., & Culver, J. P. (2017). Mapping effective connectivity within cortical networks with diffuse optical tomography. *Neurophotonics*, *4*(4), 041402. https://doi.org/10.1117/1.NPh.4.4.041402

Hassanpour, M. S., White, B. R., Eggebrecht, A. T., Ferradal, S. L., Snyder, A. Z., & Culver, J. P. (2014). Statistical analysis of high density diffuse optical tomography. *NeuroImage*, *85*, 104–116. https://doi.org/10.1016/j.neuroimage.2013.05.105

He, B. J., Snyder, A. Z., Vincent, J. L., Epstein, A., Shulman, G. L., & Corbetta, M. (2007). Breakdown of functional connectivity in frontoparietal networks underlies behavioral deficits in spatial neglect. *Neuron*, *53*(6), 905–918. https://doi.org/10.1016/j.neuron.2007.02.013

Hirai, M., Sakurada, T., Izawa, J., Ikeda, T., Monden, Y., Shimoizumi, H., & Yamagata, T. (2021). Greater reliance on proprioceptive information during a reaching task with perspective manipulation among children with autism spectrum disorders. *Scientific Reports*, *11*(1), 15974. https://doi.org/10.1038/s41598-021-95349-0

Hsu, H. M., Yao, Z. F., Hwang, K., & Hsieh, S. (2020). Between-module functional connectivity of the salient ventral attention network and dorsal attention network is associated with motor inhibition. *PLoS One*, *15*(12), e0242985. https://doi.org/10.1371/journal.pone.0242985

Iacoboni, M. (2006). Visuo-motor integration and control in the human posterior parietal cortex: Evidence from TMS and fMRI. *Neuropsychologia*, *44*(13), 2691–2699. https://doi.org/10.1016/j.neuropsychologia.2006.04.029

Iacoboni, M., & Dapretto, M. (2006). The mirror neuron system and the consequences of its dysfunction. *Nature Reviews Neuroscience*, *7*(12), 942–951. https://doi.org/10.1038/nrn2024

Iacoboni, M., Molnar-Szakacs, I., Gallese, V., Buccino, G., Mazziotta, J. C., & Rizzolatti, G. (2005). Grasping the intentions of others with one's own mirror neuron system. *PLoS Biology*, *3*(3), e79. https://doi.org/10.1371/journal.pbio.0030079

Iacoboni, M., Woods, R. P., Brass, M., Bekkering, H., Mazziotta, J. C., & Rizzolatti, G. (1999). Cortical mechanisms of human imitation. *Science*, *286*(5449), 2526–2528. https://doi.org/10.1126/science.286.5449.2526

Kana, R. K., Wadsworth, H. M., & Travers, B. G. (2011). A systems level analysis of the mirror neuron hypothesis and imitation impairments in autism spectrum disorders. *Neuroscience and Biobehavioral Reviews*, *35*(3), 894–902. https://doi.org/10.1016/j.neubiorev.2010.10.007

Kemmerer, D. (2021). What modulates the Mirror Neuron System during action observation?: Multiple factors involving the action, the actor, the observer, the relationship between actor and observer, and the

context. *Progress in Neurobiology*, *205*, 102128. https://doi.org/10.1016/j.pneurobio.2021.102128
Kilner, J. M., Marchant, J. L., & Frith, C. D. (2006). Modulation of the mirror system by social relevance. *Social Cognitive and Affective Neuroscience*, *1*(2), 143–148. https://doi.org/10.1093/scan/nsl017
Kinard, J. L., Mosner, M. G., Greene, R. K., Addicott, M., Bizzell, J., Petty, C., Cernasov, P., Walsh, E., Eisenlohr-Moul, T., Carter, R. M., McLamb, M., Hopper, A., Sukhu, R., & Dichter, G. S. (2020). Neural mechanisms of social and nonsocial reward prediction errors in adolescents with autism spectrum disorder. *Autism Research*, *13*(5), 715–728. https://doi.org/10.1002/aur.2273
Krall, S. C., Rottschy, C., Oberwelland, E., Bzdok, D., Fox, P. T., Eickhoff, S. B., Fink, G. R., & Konrad, K. (2015). The role of the right temporoparietal junction in attention and social interaction as revealed by ALE meta-analysis. *Brain Structure and Function*, *220*(2), 587–604. https://doi.org/10.1007/s00429-014-0803-z
Kruger, B., Bischoff, M., Blecker, C., Langhanns, C., Kindermann, S., Sauerbier, I., Reiser, M., Stark, R., Munzert, J., & Pilgramm, S. (2014). Parietal and premotor cortices: Activation reflects imitation accuracy during observation, delayed imitation and concurrent imitation. *NeuroImage*, *100*, 39–50. https://doi.org/10.1016/j.neuroimage.2014.05.074
Laidi, C., Boisgontier, J., Chakravarty, M. M., Hotier, S., d'Albis, M. A., Mangin, J. F., Devenyi, G. A., Delorme, R., Bolognani, F., Czech, C., Bouquet, C., Toledano, E., Bouvard, M., Gras, D., Petit, J., Mishchenko, M., Gaman, A., Scheid, I., Leboyer, M., … Houenou, J. (2017). Cerebellar anatomical alterations and attention to eyes in autism. *Scientific Reports*, *7*(1), 12008. https://doi.org/10.1038/s41598-017-11883-w
Latreche, K., Kojovic, N., Pittet, I., Natraj, S., Franchini, M., Smith, I. M., & Schaer, M. (2024). Gesture imitation performance and visual exploration in young children with autism spectrum disorder. *Journal of Autism and Developmental Disorders*. Advance online publication. https://doi.org/10.1007/s10803-024-06595-w
Licari, M. K., Alvares, G. A., Varcin, K., Evans, K. L., Cleary, D., Reid, S. L., Glasson, E. J., Bebbington, K., Reynolds, J. E., Wray, J., & Whitehouse, A. J. O. (2020). Prevalence of motor difficulties in autism spectrum disorder: Analysis of a population-based cohort. *Autism Research: Official Journal of the International Society for Autism Research*, *13*(2), 298–306. https://doi.org/10.1002/aur.2230
Lidstone, D., Rochowiak, R., Pacheco, C., Tuncgenc, B., Vidal, R., & Mostofsky, S. (2021). Automated and scalable Computerized Assessment of Motor Imitation (CAMI) in children with Autism Spectrum Disorder using a single 2D camera: A pilot study. *Research in Autism Spectrum Disorders*, *87*, 101840. https://doi.org/10.1016/j.rasd.2021.101840
Lust, J. M., van Schie, H. T., Wilson, P. H., van der Helden, J., Pelzer, B., & Steenbergen, B. (2019). Activation of mirror neuron regions is altered in developmental coordination disorder (DCD)–neurophysiological evidence using an action observation paradigm. *Frontiers in Human Neuroscience*, *13*, 232. https://doi.org/10.3389/fnhum.2019.00232
MacNeil, L. K., & Mostofsky, S. H. (2012). Specificity of dyspraxia in children with autism. *Neuropsychology*, *26*(2), 165–171. https://doi.org/10.1037/a0026955
Maenner, M. J. (2020). Prevalence of autism spectrum disorder among children aged 8 years—Autism and developmental disabilities monitoring network, 11 sites, United States, 2016. *MMWR. Surveillance Summaries*, *69*(4), 1–12. https://doi.org/10.15585/mmwr.ss6904a1
Marco, E. J., Hinkley, L. B. N., Hill, S. S., & Nagarajan, S. S. (2011). Sensory processing in autism: A review of neurophysiologic findings. *Pediatric Research*, *69*(5 Pt 2), 48R–54R. https://doi.org/10.1203/PDR.0b013e3182130c54
Marko, M. K., Crocetti, D., Hulst, T., Donchin, O., Shadmehr, R., & Mostofsky, S. H. (2015). Behavioural and neural basis of anomalous motor learning in children with autism. *Brain: A Journal of Neurology*, *138*(Pt 3), 784–797. https://doi.org/10.1093/brain/awu394
Markow, Z. E., Trobaugh, J. W., Richter, E. J., Tripathy, K., Rafferty, S. M., Svoboda, A. M., Schroeder, M. L., Burns-Yocum, T. M., Bergonzi, K. M., Chevillet, M. A., Mugler, E. M., Eggebrecht, A. T., & Culver, J. P. (2025). Ultra high density imaging arrays in diffuse optical tomography for human brain mapping improve image quality and decoding performance. *Scientific Reports*, *15*(1), 3175. https://doi.org/10.1038/s41598-025-85858-7
Marsh, L. E., & Hamilton, A. F. d. C. (2011). Dissociation of mirroring and mentalising systems in autism. *NeuroImage*, *56*(3), 1511–1519. https://doi.org/10.1016/j.neuroimage.2011.02.003
McAuliffe, D., Zhao, Y., Pillai, A. S., Ament, K., Adamek, J., Caffo, B. S., Mostofsky, S. H., & Ewen, J. B. (2020). Learning of skilled movements via imitation in ASD. *Autism Research: Official Journal of the International Society for Autism Research*, *13*(5), 777–784. https://doi.org/10.1002/aur.2253
McMorrow, S. R., Park, S. M., George, T. G., Sobolewski, C. M., Yang, D. L., King, K. T., Kenley, J., Smyser, C. D., Culver, J. P., Guilliams, K. P., Said, A. S., & Eggebrecht, A. T. (2025). Bedside neuroimaging using high-density diffuse optical tomography in a pediatric patient on extracorporeal support. *Stroke*, *56*(1), e3–e5. https://doi.org/10.1161/Strokeaha.124.049116
Michalowski, B., Buchwald, M., Klichowski, M., Ras, M., & Kroliczak, G. (2022). Action goals and the praxis network: An fMRI study. *Brain Structure & Function*, *227*(7), 2261–2284. https://doi.org/10.1007/s00429-022-02520-y
Miller, H. L., Licari, M. K., Bhat, A., Aziz-Zadeh, L. S., Van Damme, T., Fears, N. E., Cermak, S. A., & Tamplain, P. M. (2024). Motor problems in autism: Co-occurrence or feature? *Developmental Medicine and Child Neurology*, *66*(1), 16–22. https://doi.org/10.1111/dmcn.15674
Miller, H. L., Sherrod, G. M., Mauk, J. E., Fears, N. E., Hynan, L. S., & Tamplain, P. M. (2021). Shared features or co-occurrence? Evaluating symptoms of developmental coordination disorder in children and adolescents with autism spectrum disorder. *Journal of Autism and Developmental Disorders*, *51*(10), 3443–3455. https://doi.org/10.1007/s10803-020-04766-z
Mishra, W., Kheradpezhouh, E., & Arabzadeh, E. (2024). Activation of M1 cholinergic receptors in mouse somatosensory cortex enhances information processing and detection behaviour. *Communications Biology*, *7*(1), 3. https://doi.org/10.1038/s42003-023-05699-w
Mizuguchi, N., Nakata, H., & Kanosue, K. (2016). The right temporoparietal junction encodes efforts of others during action observation. *Scientific Reports*, *6*, 30274. https://doi.org/10.1038/srep30274
Mostofsky, S. H., Dubey, P., Jerath, V. K., Jansiewicz, E. M., Goldberg, M. C., & Denckla, M. B. (2006). Developmental dyspraxia is not limited to imitation in children with autism spectrum disorders. *Journal of the International Neuropsychological Society: JINS*, *12*(3), 314–326. https://doi.org/10.1017/s1355617706060437
Mottron, L., & Bzdok, D. (2020). Autism spectrum heterogeneity: Fact or artifact? *Molecular Psychiatry*, *25*(12), 3178–3185. https://doi.org/10.1038/s41380-020-0748-y

Nachev, P., Wydell, H., O'Neill, K., Husain, M., & Kennard, C. (2007). The role of the pre-supplementary motor area in the control of action. *NeuroImage*, *36*(Suppl. 2, 3–3), T155–T163. https://doi.org/10.1016/j.neuroimage.2007.03.034

Nardo, D., Santangelo, V., & Macaluso, E. (2011). Stimulus-driven orienting of visuo-spatial attention in complex dynamic environments. *Neuron*, *69*(5), 1015–1028. https://doi.org/10.1016/j.neuron.2011.02.020

Nebel, M. B., Eloyan, A., Nettles, C. A., Sweeney, K. L., Ament, K., Ward, R. E., Choe, A. S., Barber, A. D., Pekar, J. J., & Mostofsky, S. H. (2016). Intrinsic visual-motor synchrony correlates with social deficits in autism. *Biological Psychiatry*, *79*(8), 633–641. https://doi.org/10.1016/j.biopsych.2015.08.029

Oberman, L. M., Ramachandran, V. S., & Pineda, J. A. (2008). Modulation of mu suppression in children with autism spectrum disorders in response to familiar or unfamiliar stimuli: The mirror neuron hypothesis. *Neuropsychologia*, *46*(5), 1558–1565. https://doi.org/10.1016/j.neuropsychologia.2008.01.010

Oldfield, R. C. (1971). The assessment and analysis of handedness: The Edinburgh inventory. *Neuropsychologia*, *9*(1), 97–113. https://doi.org/10.1016/0028-3932(71)90067-4

Orban, G. A., Sepe, A., & Bonini, L. (2021). Parietal maps of visual signals for bodily action planning. *Brain Structure and Function*, *226*(9), 2967–2988. https://doi.org/10.1007/s00429-021-02378-6

Ozonoff, S., Pennington, B. F., & Rogers, S. J. (1991). Executive function deficits in high-functioning autistic individuals: Relationship to theory of mind. *Journal of Child Psychology and Psychiatry*, *32*(7), 1081–1105. https://doi.org/10.1111/j.1469-7610.1991.tb00351.x

Papadatou-Pastou, M., Ntolka, E., Schmitz, J., Martin, M., Munafo, M. R., Ocklenburg, S., & Paracchini, S. (2020). Human handedness: A meta-analysis. *Psychological Bulletin*, *146*(6), 481–524. https://doi.org/10.1037/bul0000229

Picard, N., Matsuzaka, Y., & Strick, P. L. (2013). Extended practice of a motor skill is associated with reduced metabolic activity in M1. *Nature Neuroscience*, *16*(9), 1340–1347. https://doi.org/10.1038/nn.3477

Pittet, I., Kojovic, N., Franchini, M., & Schaer, M. (2022). Trajectories of imitation skills in preschoolers with autism spectrum disorders. *Journal of Neurodevelopmental Disorders*, *14*(1), 2. https://doi.org/10.1186/s11689-021-09412-y

Pitts, C. H., & Mervis, C. B. (2016). Performance on the kaufman brief intelligence test-2 by children with williams syndrome. *American Association on Intellectual and Developmental Disabilities*, *121*(1), 33–47. https://doi.org/10.1352/1944-7558-121.1.33

Raymaekers, R., Wiersema, J. R., & Roeyers, H. (2009). EEG study of the mirror neuron system in children with high functioning autism. *Brain Research*, *1304*, 113–121. https://doi.org/10.1016/j.brainres.2009.09.068

Rizzolatti, G., & Craighero, L. (2004). The mirror-neuron system. *Annual Review of Neuroscience*, *27*(1), 169–192. https://doi.org/10.1146/annurev.neuro.27.070203.144230

Rizzolatti, G., & Fabbri-Destro, M. (2008). The mirror system and its role in social cognition. *Current Opinion in Neurobiology*, *18*(2), 179–184. https://doi.org/10.1016/j.conb.2008.08.001

Rogers, S. J., & Vismara, L. A. (2008). Evidence-based comprehensive treatments for early autism. *Journal of Clinical Child & Adolescent Psychology*, *37*(1), 8–38. https://doi.org/10.1080/15374410701817808

Rosenzopf, H., Wiesen, D., Basilakos, A., Yourganov, G., Bonilha, L., Rorden, C., Fridriksson, J., Karnath, H. O., & Sperber, C. (2022). Mapping the human praxis network: An investigation of white matter disconnection in limb apraxia of gesture production. *Brain Communications*, *4*(1), fcac004. https://doi.org/10.1093/braincomms/fcac004

Sadato, N., Yonekura, Y., Waki, A., Yamada, H., & Ishii, Y. (1997). Role of the supplementary motor area and the right premotor cortex in the coordination of bimanual finger movements. *The Journal of Neuroscience*, *17*(24), 9667–9674. https://doi.org/10.1523/JNEUROSCI.17-24-09667.1997

Santra, R., Pacheco, C., Crocetti, D., Vidal, R., Mostofsky, S. H., & Tunçgenç, B. (2025). Evaluating computerised assessment of motor imitation (CAMI) for identifying autism-specific difficulties not observed for attention-deficit hyperactivity disorder or neurotypical development. *The British Journal of Psychiatry*, 1–8. Advance online publication. https://doi.org/10.1192/bjp.2024.235

Scarapicchia, V., Brown, C., Mayo, C., & Gawryluk, J. R. (2017). Functional magnetic resonance imaging and functional near-infrared spectroscopy: Insights from combined recording studies. *Frontiers in Human Neuroscience*, *11*, 419. https://doi.org/10.3389/fnhum.2017.00419

Scassellati, B. (1999). Imitation and mechanisms of joint attention: A developmental structure for building social skills on a humanoid robot. In C. L. Nehaniv (Ed.), *Computation for metaphors, analogy, and agents* (Vol. *1562*, pp. 176–195). Springer. https://doi.org/10.1007/3-540-48834-0_11

Schroeder, M. L., Sherafati, A., Ulbrich, R. L., Wheelock, M. D., Svoboda, A. M., Klein, E. D., George, T. G., Tripathy, K., Culver, J. P., & Eggebrecht, A. T. (2023). Mapping cortical activations underlying covert and overt language production using high-density diffuse optical tomography. *NeuroImage*, *276*, 120190. https://doi.org/10.1016/j.neuroimage.2023.120190

Sherafati, A., Snyder, A. Z., Eggebrecht, A. T., Bergonzi, K. M., Burns-Yocum, T. M., Lugar, H. M., Ferradal, S. L., Robichaux-Viehoever, A., Smyser, C. D., Palanca, B. J., Hershey, T., & Culver, J. P. (2020). Global motion detection and censoring in high-density diffuse optical tomography. *Human Brain Mapping*, *41*(14), 4093–4112. https://doi.org/10.1002/hbm.25111

Sowden, S., & Catmur, C. (2015). The role of the right temporoparietal junction in the control of imitation. *Cerebral Cortex*, *25*(4), 1107–1113. https://doi.org/10.1093/cercor/bht306

Su, W. C., Culotta, M., Mueller, J., Tsuzuki, D., & Bhat, A. N. (2023). Autism-related differences in cortical activation when observing, producing, and imitating communicative gestures: An fNIRS study. *Brain Sciences*, *13*(9), 1284. https://doi.org/10.3390/brainsci13091284

Su, W. C., Culotta, M., Mueller, J., Tsuzuki, D., Pelphrey, K., & Bhat, A. (2020). Differences in cortical activation patterns during action observation, action execution, and interpersonal synchrony between children with or without autism spectrum disorder (ASD): An fNIRS pilot study. *PLoS One*, *15*(10), e0240301. https://doi.org/10.1371/journal.pone.0240301

Taverna, E. C., Huedo-Medina, T. B., Fein, D. A., & Eigsti, I.-M. (2021). The interaction of fine motor, gesture, and structural language skills: The case of autism spectrum disorder. *Research in Autism Spectrum Disorders*, *86*, 101824. https://doi.org/10.1016/j.rasd.2021.101824

Tripathy, K., Fogarty, M., Svoboda, A. M., Schroeder, M. L., Rafferty, S. M., Richter, E. J., Tracy, C., Mansfield, P. K., Booth, M., Fishell, A. K., Sherafati, A., Markow, Z. E., Wheelock, M. D., Arbelaez, A. M., Schlaggar, B. L., Smyser, C. D., Eggebrecht, A. T., & Culver, J. P. (2024). Mapping brain function in adults and young children during naturalistic viewing with high-density diffuse optical tomography. *Human Brain Mapping*, *45*(7), e26684. https://doi.org/10.1002/hbm.26684

Tuncgenc, B., Pacheco, C., Rochowiak, R., Nicholas, R., Rengarajan, S., Zou, E., Messenger, B., Vidal, R., & Mostofsky, S. H. (2021). Computerized assessment of motor imitation as a scalable method for distinguishing children with autism. *Biological Psychiatry: Cognitive Neuroscience and Neuroimaging*, *6*(3), 321–328. https://doi.org/10.1016/j.bpsc.2020.09.001

Tylen, K., Allen, M., Hunter, B., & Roepstorff, A. (2012). Interaction vs. observation: Distinctive modes of social cognition in human brain and behavior? A combined fMRI and eye-tracking study. *Frontiers in Human Neuroscience*, *6*, 331. https://doi.org/10.3389/fnhum.2012.00331

Uchitel, J., Blanco, B., Collins-Jones, L., Edwards, A., Porter, E., Pammenter, K., Hebden, J., Cooper, R. J., & Austin, T. (2023). Cot-side imaging of functional connectivity in the developing brain during sleep using wearable high-density diffuse optical tomography. *NeuroImage*, *265*, 119784. https://doi.org/10.1016/j.neuroimage.2022.119784

Uchitel, J., Blanco, B., Vidal-Rosas, E., Collins-Jones, L., & Cooper, R. J. (2022). Reliability and similarity of resting state functional connectivity networks imaged using wearable, high-density diffuse optical tomography in the home setting. *NeuroImage*, *263*, 119663. https://doi.org/10.1016/j.neuroimage.2022.119663

Umiltà, M. A., Kohler, E., Gallese, V., Fogassi, L., Fadiga, L., Keysers, C., & Rizzolatti, G. (2001). I know what you are doing: A neurophysiological study. *Neuron*, *31*(1), 155–165. https://doi.org/10.1016/S0896-6273(01)00337-3

Villalobos, M. E., Mizuno, A., Dahl, B. C., Kemmotsu, N., & Müller, R.-A. (2005). Reduced functional connectivity between V1 and inferior frontal cortex associated with visuomotor performance in autism. *NeuroImage*, *25*(3), 916–925. https://doi.org/10.1016/j.neuroimage.2004.12.022

Vivanti, G., & Hamilton, A. (2014). Imitation in autism spectrum disorders. In F. R. Volkmar, S. J. Rogers, R. Paul, & K. A. Pelphrey (Eds.), *Handbook of autism and pervasive developmental disorders: Diagnosis, development, and brain mechanisms* (4th ed., pp. 278–301). John Wiley & Sons, Inc.. ISBN: 978-1-118-28219-9

Vossel, S., Geng, J. J., & Fink, G. R. (2014). Dorsal and ventral attention systems: Distinct neural circuits but collaborative roles. *The Neuroscientist*, *20*(2), 150–159. https://doi.org/10.1177/1073858413494269

Wadsworth, H. M., Maximo, J. O., Donnelly, R. J., & Kana, R. K. (2018). Action simulation and mirroring in children with autism spectrum disorders. *Behavioural Brain Research*, *341*, 1–8. https://doi.org/10.1016/j.bbr.2017.12.012

White, B. R., & Culver, J. P. (2010). Quantitative evaluation of high-density diffuse optical tomography: In vivo resolution and mapping performance. *Journal of Biomedical Optics*, *15*(2), 026006. https://doi.org/10.1117/1.3368999

Williams, J. H. G., Whiten, A., Suddendorf, T., & Perrett, D. I. (2001). Imitation, mirror neurons and autism. *Neuroscience and Biobehavioral Reviews*, *25*(4), 287–295. https://doi.org/10.1016/S0149-7634(01)00014-8

Wymbs, N. F., Nebel, M. B., Ewen, J. B., & Mostofsky, S. H. (2021). Altered inferior parietal functional connectivity is correlated with praxis and social skill performance in children with autism spectrum disorder. *Cerebral Cortex*, *31*(5), 2639–2652. https://doi.org/10.1093/cercor/bhaa380

Yang, D., Sidman, J., & Bushnell, E. W. (2010). Beyond the information given: Infants' transfer of actions learned through imitation. *Journal of Experimental Child Psychology*, *106*(1), 62–81. https://doi.org/10.1016/j.jecp.2009.12.005

Yang, D., Svoboda, A. M., George, T. G., Mansfield, P. K., Wheelock, M. D., Schroeder, M. L., Rafferty, S. M., Sherafati, A., Tripathy, K., Burns-Yocum, T., Forsen, E., Pruett, J. R., Marrus, N. M., Culver, J. P., Constantino, J. N., & Eggebrecht, A. T. (2024). Mapping neural correlates of biological motion perception in autistic children using high-density diffuse optical tomography. *Molecular Autism*, *15*(1), 35. https://doi.org/10.1186/s13229-024-00614-4

Yucel, M. A., Luhmann, A. V., Scholkmann, F., Gervain, J., Dan, I., Ayaz, H., Boas, D., Cooper, R. J., Culver, J., Elwell, C. E., Eggebrecht, A., Franceschini, M. A., Grova, C., Homae, F., Lesage, F., Obrig, H., Tachtsidis, I., Tak, S., Tong, Y., … Wolf, M. (2021). Best practices for fNIRS publications. *Neurophotonics*, *8*(1), 012101. https://doi.org/10.1117/1.NPh.8.1.012101

Zeff, B. W., White, B. R., Dehghani, H., Schlaggar, B. L., & Culver, J. P. (2007). Retinotopic mapping of adult human visual cortex with high-density diffuse optical tomography. *Proceedings of the National Academy of Sciences of the United States of America*, *104*(29), 12169–12174. https://doi.org/10.1073/pnas.0611266104

Zhao, W., Liu, Q., Zhang, X., Song, X., Zhang, Z., Qing, P., Liu, X., Zhu, S., Yang, W., & Kendrick, K. M. (2023). Differential responses in the mirror neuron system during imitation of individual emotional facial expressions and association with autistic traits. *NeuroImage*, *277*, 120263. https://doi.org/10.1016/j.neuroimage.2023.120263